Title

A Disulfide-Stabilized Aβ that Forms Dimers but Does Not Form Fibrils.

Journal

Biochemistry, 61(4)

Authors

Zhang, Sheng

Yoo, Stan

Snyder, Dalton

et al.

Publication Date

2022-02-15

DOI

10.1021/acs.biochem.1c00739

Peer reviewed

HHS Public Access

Author manuscript

Biochemistry. Author manuscript; available in PMC 2023 February 15.

Published in final edited form as:

Biochemistry. 2022 February 15; 61(4): 252–264. doi:10.1021/acs.biochem.1c00739.

A Disulfide-Stabilized Aβ That Forms Dimers But Does Not Form Fibrils

Sheng Zhang[1], **Stan Yoo**[1], **Dalton T. Snyder**[3], **Benjamin B. Katz**[1], **Amy Henrickson**[4], **Borries Demeler**[4], **Vicki H. Wysocki**[3], **Adam G. Kreutzer**[1,*], **James S. Nowick**[1,2,*]

[1]Department of Chemistry, University of California Irvine, Irvine, California 92697-2025, United States

[2]Department of Pharmaceutical Sciences, University of California Irvine, Irvine, California 92697-2025, United States

[3]Resource for Native Mass Spectrometry Guided Structural Biology, The Ohio State University, Columbus, Ohio 43210, United States

[4]Department of Chemistry and Biochemistry, University of Lethbridge, 4401 University Dr., Lethbridge, Alberta, Canada T1K 3M4

Abstract

Aβ dimers are a basic building block of many larger Aβ oligomers and are among the most neurotoxic and pathologically relevant species in Alzheimer's disease. Homogeneous Aβ dimers are difficult to prepare, characterize and study, because Aβ forms heterogeneous mixtures of oligomers that vary in size and can rapidly aggregate into more stable fibrils. This paper introduces $Aβ_{C18C33}$ as a disulfide-stabilized analogue of $Aβ_{42}$ that forms stable homogeneous dimers in lipid environments but does not aggregate to form insoluble fibrils. The $Aβ_{C18C33}$ peptide is readily expressed in *E. coli* and purified by reverse-phase HPLC to give ca. 8 mg of pure peptide per liter of bacterial culture. SDS-PAGE establishes that $Aβ_{C18C33}$ forms homogeneous dimers in the membrane-like environment of SDS and that conformational stabilization of the peptide with a disulfide bond prevents the formation of heterogeneous mixtures of oligomers. Mass spectrometric studies in the presence of dodecyl maltoside (DDM) further confirm the formation of stable noncovalent dimers. Circular dichroism (CD) spectroscopy establishes that $Aβ_{C18C33}$ adopts a β-sheet conformation in detergent solutions and supports a model in which the intramolecular disulfide bond induces β-hairpin folding and dimer formation in lipid environments. Thioflavin T fluorescence assays and transmission electron microscopy (TEM) studies indicate that $Aβ_{C18C33}$ does not undergo fibril formation in aqueous buffer solutions

[*]**Corresponding Authors**: James S. Nowick – Department of Chemistry, University of California, Irvine, California 92697-2025, United States; Department of Pharmaceutical Sciences, University of California, Irvine, California 92697-2025, United States. jsnowick@uci.edu, Adam G. Kreutzer – Department of Chemistry, University of California, Irvine, California 92697-2025, United States. akreutze@uci.edu.

Supporting Information

The Supporting Information is available free of charge on the ACS Publications website at http://pubs.acs.org.

Detailed procedures for molecular cloning, peptide expression, purification, and characterization, as well as SDS-PAGE, mass spectrometry, CD, ThT, TEM, AUC, and DLS studies. Supplementary figures and tables, and characterization data for the expressed peptides.

The authors declare no competing financial interest.

and demonstrate that the intramolecular disulfide bond prevents fibril formation. The recently published NMR structure of an $A\beta_{42}$ tetramer (PDB 6RHY) provides a working model for the $A\beta_{C18C33}$ dimer, in which two β-hairpins assemble through hydrogen bonding to form a four-stranded antiparallel β-sheet. It is anticipated that $A\beta_{C18C33}$ will serve as a stable, nonfibrilizing, noncovalent Aβ dimer model for amyloid and Alzheimer's disease research.

Graphical Abstract

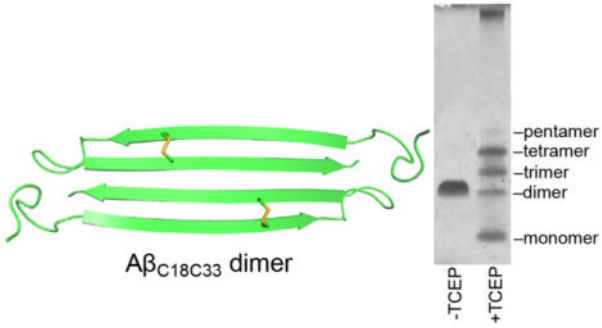

Introduction

Dimers are among the most important oligomers of the β-amyloid peptide, Aβ. Although Aβ fibrils are the most commonly found Aβ species in Alzheimer's disease brains, Aβ oligomers are key contributors to neurodegeneration.[1–6] Small oligomers of Aβ have been shown to be far more neurotoxic than large oligomers.[7–9] Aβ dimers are thought to be the basic building block of many larger Aβ oligomers and are one of the most neurotoxic and pathologically relevant species in Alzheimer's disease.[10–18] Homogeneous Aβ dimers are difficult to prepare, characterize and study, because Aβ forms heterogeneous mixtures of oligomers that vary in size and can rapidly aggregate into more stable fibrils.[19–27] A plentiful source of homogeneous and stable Aβ dimers would be valuable in amyloid and Alzheimer's disease research.

Although biogenic Aβ oligomers are arguably more biologically relevant than synthetic Aβ oligomers, biogenic Aβ oligomers are difficult to study because they only occur in minute concentrations and must be isolated from brain tissue.[7,12–15,28] When Aβ oligomers are prepared by allowing Aβ to aggregate in vitro, the resulting Aβ oligomers are heterogeneous in size, morphology, and toxicity.[29,30] To obtain Aβ dimers, researchers have covalently crosslinked Aβ monomers through several types of intermolecular linkages, including isopeptide bonds,[28,31,32] dityrosine bonds,[28,31,33–35] disulfide bonds,[16,18,34,36–38] homocysteine disulfide bonds,[38] glycine–serine-rich linkers,[39,40] alkyl linkers,[38,41–43] 4-hydroxynonenal induced crosslinking,[44] and photoinduced crosslinking of unmodified proteins (PICUP).[23,24,45–47] These covalent Aβ dimers generally aggregate further with time into a heterogeneous mixture of larger oligomers, protofibrils, or fibrils (Table S8).

Noncovalent Aβ dimers may be more biologically relevant than covalent dimers, because they mimic native Aβ dimers that are formed through noncovalent interactions (Figure 1).[5,33,48–50] Previous approaches to generate noncovalent oligomers have relied upon

stabilizing intramolecular linkages, including intramolecular disulfide bonds and oxime linkages, to facilitate noncovalent Aβ oligomer formation.[51–57] These intramolecular linkages are designed to induce a β-hairpin conformation, stabilizing Aβ in the oligomeric state and thus delaying or preventing fibril formation. Aβ β-hairpins are thought to be the building blocks of many Aβ oligomers, and are thus of special biological relevance.[52,54,57–59] These modified Aβ peptides bearing intramolecular linkages form various sizes of oligomers upon incubation in solution (Table S8).

Aβ oligomers formed by full-length Aβ peptides bearing intermolecular or intramolecular linkages have proven useful in amyloid and Alzheimer's disease research.[60–64] These artificial oligomers have been used as chemical models to study a variety of aspects of Aβ oligomers, including neurotoxicity,[16,37,38,41,51,52,55] aggregation kinetics and pathways,[23,24,28,31–34,36,42,44,52,56] effects on behavioral deficits and neuroplasticity,[18] antibody-binding activities,[43,57] and oligomer structures.[53] Even though these efforts have provided useful chemical model systems, most of the oligomers produced are heterogeneous mixtures comprising multiple oligomerization states. There are, to our knowledge, no model systems based on full-length Aβ that form stable homogeneous dimers.

Our laboratory has recently developed conditions that permit the efficient expression and purification of $A\beta_{42}$ peptides and mutants thereof.[65,66] In the current study, we set out to explore the effect of intramolecular disulfide linkages in $A\beta_{42}$ peptides, by preparing and studying a variety of mutant $A\beta_{42}$ peptides containing two cysteine residues. Here, we report the discovery and preparation of $A\beta_{C18C33}$, a mutant $A\beta_{42}$ peptide containing an intramolecular disulfide bond that forms stable homogeneous dimers in lipid environments.

Materials and Methods

The materials and procedures for molecular cloning, peptide expression, purification, and characterization, as well as SDS-PAGE, mass spectrometry, CD, ThT, TEM, AUC, and DLS studies are described in detail in the Supporting Information.

Results and Discussion

Design of Disulfide-Stabilized $A\beta_{42}$ Peptides.

In previous studies, our laboratory has observed that β-hairpin peptides derived from Aβ that contain different residue pairings from the central and C-terminal regions of Aβ form different types of oligomeric assemblies.[67] Inspired by this observation, as well as by earlier studies of Aβ peptides containing disulfide linkages,[51–53,57] we expressed and purified five mutant $A\beta_{42}$ peptides containing pairs of cysteine residues at positions 21 and 30, 18 and 33, 21 and 32, 24 and 29, and 21 and 31, respectively (Figure 2). In each peptide, we mutated one nonpolar residue from the hydrophobic central region of Aβ and one nonpolar residue from the hydrophobic C-terminal region, with the goal of inducing β-hairpin formation with different residue pairings or hydrogen-bonding patterns. For example, while peptides $A\beta_{C21C30}$ and $A\beta_{C18C33}$ share the same residue pairing, the peptides differ in hydrogen-bonding pattern. In peptide $A\beta_{C21C30}$, amino acids K_{16}, V_{18}, F_{20}, and E_{22} hydrogen bond with amino acids M_{35}, G_{33}, I_{31}, and G_{29}, while in peptide $A\beta_{C18C33}$, amino acids Q_{15}, L_{17},

F_{19}, A_{21}, and D_{23} hydrogen bond with amino acids V_{36}, L_{34}, I_{32}, A_{30}, and K_{28}. $A\beta_{C21C30}$ has previously been reported to form a mixture of dimers and trimers in SDS-PAGE and hexamers in the solid state.[52,53] The other four peptides, $A\beta_{C18C33}$, $A\beta_{C21C32}$, $A\beta_{C24C29}$, and $A\beta_{C21C31}$, have not been previously reported.

Preparation of Disulfide-Stabilized Aβ Peptides.

We prepared the mutant Aβ peptides by expression in *E. coli* followed by reverse-phase HPLC purification.[65,66] We first prepared the corresponding recombinant plasmids encoding mutant Aβ peptides bearing double cysteine mutations through molecular cloning (Figure S1 and S2). We then transformed the recombinant plasmids into *E. coli* and expressed the mutant Aβ peptides through isopropyl β-D-1-thiogalactopyranoside (TPTG) induction. After expression, we lysed the cells and solubilized the inclusion bodies with urea to obtain cell lysate containing the mutant Aβ peptides. We then added dimethyl sulfoxide (DMSO) to the cell lysate to oxidize the cysteines to form the intramolecular disulfide bond in each mutant Aβ peptide. Finally, we purified the disulfide-stabilized Aβ peptides by preparative reverse-phase HPLC using a C8 column at 80 °C with water and acetonitrile containing 0.1% trifluoroacetic acid (TFA). This procedure afforded ca. 8 mg of each pure mutant peptide from one liter of bacterial culture (Table S7). Each of the peptides contains an N-terminal methionine residue, that results from the start codon for the expression. For comparison, we also prepared $A\beta_{(M1–42)}$, which is a homologue of full-length $A\beta_{42}$ with properties similar to native $A\beta_{42}$.[65,68]

SDS-PAGE Studies of the Mutant $A\beta_{42}$ Peptides: Discovery of the $A\beta_{C18C33}$ Dimer.

To evaluate the propensities of the disulfide-stabilized Aβ peptides to form oligomers, we performed sodium dodecyl sulfate-polyacrylamide gel electrophoresis (SDS-PAGE) and used silver staining to visualize the species formed by each peptide (Figure 3A). Tn the SDS-PAGE, $A\beta_{(M1–42)}$ runs with the main band just above the 5 kDa ladder band, at ca. 6 kDa, which corresponds to the monomer, as well as a pair of weaker bands at ca. 13 kDa and 15 kDa, which are generally attributed to trimer and tetramer.[69,70] The previously reported $A\beta_{C21C30}$ peptide gives a pair of bands, with similar appearance but slightly lower in position. These bands have previously been attributed to dimer and trimer,[52] although the trimer and tetramer cannot be rigorously excluded. The $A\beta_{C21C32}$ and $A\beta_{C21C31}$ peptides give bands just above the 5 kDa ladder band, at ca. 6 kDa, and thus form monomers. The $A\beta_{C24C29}$ peptide gives a pattern of monomer, trimer, and tetramer bands similar in position and appearance to those of $A\beta_{(M1–42)}$. The $A\beta_{C18C33}$ peptide stands out among the mutant peptides, giving an intense band midway between the 10 and 15 kDa ladder bands, at ca. 12 kDa, which corresponds to a dimer.

To further explore the dimerization of the $A\beta_{C18C33}$ peptide, we ran SDS-PAGE at concentrations ranging from 7.8 to 500 μM (Figure 3B). At each concentration, the dimer band predominates, with small bands corresponding to monomer, and higher-order oligomers appearing at higher concentrations. In contrast, $A\beta_{(M1–42)}$ shows a predominance of the monomer at all concentrations, with the trimer and tetramer bands appearing at higher concentrations.

To investigate the effect of the disulfide bond of $A\beta_{C18C33}$ upon dimer formation, we reduced the disulfide bond with tris(2-carboxyethyl)phosphine hydrochloride (TCEP) and studied the oligomerization of the reduced $A\beta_{C18C33}$ peptide by SDS-PAGE (Figure 4). The reduced $A\beta_{C18C33}$ peptide behaves more like $A\beta_{(M1–42)}$, showing distinct bands corresponding to monomer, dimer, trimer, and tetramer, at lower concentrations, as well as an additional band corresponding to a pentamer at higher concentrations. The reduced $A\beta_{C18C33}$ peptide also shows a band at the very top of the gel, indicating that the reduced peptide also assembles to form fibrils or other high-molecular-weight aggregates. These results demonstrate that the disulfide bond is essential for homogeneous dimer formation and establish that the cysteine mutations alone do not induce the formation of a pronounced dimer band in SDS-PAGE.

Mass Spectrometric Studies of $A\beta_{C18C33}$.

To further corroborate the formation of noncovalent dimers and to exclude the possibility of covalent dimer formation through a pair of intermolecular disulfide bonds, we performed mass spectrometry. Matrix-assisted laser desorption/ionization (MALDT) mass spectrometry shows exclusively the $A\beta_{C18C33}$ monomer (Figure S14). This observation is significant, because it establishes that the dimer observed for $A\beta_{C18C33}$ in SDS-PAGE is non-covalent, rather than a catenane or a covalent dimer formed through a pair of intermolecular disulfide bonds. The $A\beta_{C18C33}$ peptide also shows monomer in the ESI mass spectrum in SEC-MS, eluting with ammonium formate and acetonitrile at pH 10 (Figure 5A). Incubation of $A\beta_{C18C33}$ with the non-ionic detergent dodecyl maltoside (DDM), followed SEC-MS analysis, gives a new peak in the total ion current chromatogram associated with the dimer (Figure 5B). Analysis of this chromatographic peak reveals $[\text{dimer} + 5H]^{5+}$ and $[\text{dimer} + 6H]^{6+}$ ions associated with the dimer (Figure 5C and 5D). The observation of noncovalent dimers in SEC-MS experiments with DDM provides further evidence that $A\beta_{C18C33}$ forms well-defined dimers in the presence of detergent.

To further characterize the noncovalent $A\beta_{C18C33}$ dimers, we performed native ion mobility-mass spectrometry (IM-MS).[70] In this technique, the sample is directly injected into the mass spectrometer, and species are separated in the gas phase on the basis of mobility and then mass-to-charge ratio. A solution of 25 μM $A\beta_{C18C33}$ and 300 μM DDM in 200 mM ammonium acetate buffer at pH 7.4 directly injected into the instrument gave an ion mobility chromatogram with two main peaks with arrival times at 7.8 and 11.1 ms (Figure 6). Analysis of the isotope patterns and m/z ratios of the mass spectrometric peaks associated with the 7.8-ms ion mobility peak revealed a distinct signature for the $[\text{dimer} + 4H]^{4+}$, indicating that this peak corresponds to the dimer. Similar analysis of the 11.2-ms ion mobility peak revealed a distinct signature for the $[\text{monomer} + 2H]^{2+}$, indicating that this peak corresponds to the monomer. The SEC-MS and IM-MS results thus agree with SDS-PAGE results that $A\beta_{C18C33}$ forms well-defined dimers in the presence of detergent micelles.

We conducted high-resolution native mass spectrometry on an Orbitrap Exactive Ultrahigh Mass Range (UHMR) mass spectrometer — a high-sensitivity instrument with excellent mass range and high m/z transmission — to provide additional insights into the dimers

formed by $A\beta_{C18C33}$ in DDM. When solutions of $A\beta_{(M1–42)}$ in 200 mM ammonium acetate were nanoelectrosprayed into the instrument, only monomers were observed, regardless of whether 300 μM DDM was included (Figure 7C and 7D).

$A\beta_{C18C33}$ exhibits very different behavior than $A\beta_{(M1–42)}$ in high-resolution native mass spectrometry. When a solution of $A\beta_{C18C33}$ in 200 mM ammonium acetate (without DDM) was nanoelectrosprayed into the instrument, monomers and tetramers were observed, with the monomer peaks having substantially greater intensity than the tetramer peaks (Figure 7A). The peaks for the monomers and the tetramers each appear as broad ladders, reflecting the presence of multiple sodium ions, which likely arise from the sodium hydroxide treatment during the preparation of the Aβ. The stoichiometry of the tetramers was confirmed by MS/MS, which produced monomer and trimer fragment ions (data not shown).

Inclusion of DDM in the $A\beta_{C18C33}$ sample resulted in the formation of dimers. When a solution of $A\beta_{C18C33}$ in 200 mM ammonium acetate containing 300 μM DDM was nanoelectrosprayed into the instrument, dimers and tetramers were observed, with little or no monomer (Figure 7B). The dimers and tetramers were observed as DDM adducts, with 2–3 DDM molecules per dimer and 6 DDM molecules per tetramer. All species were assigned based on charge states from isotopic patterns available using the 100,000-resolution setting on the UHMR.

To confirm the presence of $A\beta_{C18C33}$ in the broad ladders observed in ammonium acetate containing DDM, we collected native mass spectra with collision-induced dissociation (CID) at increasing collision voltages on the Orbitrap Exactive UHMR instrument (Figure 8). Collision-induced dissociation of the entire distribution of dimers and tetramers was accomplished in the higher energy C-trap dissociation (HCD) cell.[71] At low HCD energy (e.g., 20–50 V), broad ladders corresponding to dimers and tetramers were observed. As the HCD energy was increased to 80 V and beyond, the dimers and tetramers decreased in relative abundance, concurrent with an increase in monomer abundance. The monomers have sharper features, and are thus especially easy to discern. The increase in HCD energy causes disruption of the noncovalent interactions within the dimer and tetramer complexes and dissociation to monomers, providing evidence that these broad features do contain $A\beta_{C18C33}$ peptides. Mass spectra were recorded at high resolution so that isotope spacings could be used to confidently assign charge states and thus stoichiometry. The fact that the dimer and tetramer remain adducted with several molecules of DDM in the gas phase even with significant gas-phase collisional activation is noteworthy, in that it suggests strong association of these oligomers with the DDM detergent. Interestingly, the DDM molecules are lost only when the noncovalent dimer and tetramer dissociate to monomers.

Circular Dichroism Studies of $A\beta_{C18C33}$.

To explore the structure of the dimers formed by $A\beta_{C18C33}$, we turned to circular dichroism (CD) spectroscopy. In the absence of SDS, a 30 μM solution of $A\beta_{C18C33}$ in 10 mM sodium phosphate buffer at pH 7.4 exhibits a broad negative band below 230 nm, with a shallow minimum at 203 nm (Figure 9A). With 20 mM SDS, the CD spectrum displays a well-defined minimum at 212 nm and maximum at 191 nm (Figure 9A). These data indicate that the $A\beta_{C18C33}$ peptide adopts β-sheet structure in the presence of SDS, but that

random coil structure predominates in the absence of SDS. The spectrum in the presence of SDS differs dramatically from that of $A\beta_{(M1–42)}$, which exhibits minima at 207 and 222 nm and a maximum at 190 nm in SDS and thus adopts an a-helical structure (Figure 9B). These results highlight the effect of the disulfide bond upon the conformation of $A\beta_{C18C33}$, preventing a-helix formation and enforcing β-sheet formation under conditions most relevant to SDS-PAGE.

To gain further insight into the structure of the $A\beta_{C18C33}$ dimers under conditions relevant to the mass spectrometric experiments described above, we collected CD spectra of $A\beta_{C18C33}$ and $A\beta_{(M1–42)}$ with various concentrations of DDM. The CD spectra of $A\beta_{C18C33}$ with DDM at concentrations well above the critical micelle concentration (CMC, 0.17 mM) resemble the CD spectrum of $A\beta_{C18C33}$ with 20 mM SDS (CMC 8 mM), exhibiting a well-defined minimum at 214 nm and a maximum at ca. 190 nm (Figure 10A). The CD spectrum of $A\beta_{(M1–42)}$ with DDM displays a broader minimum, centered at 215 nm, and a weaker maximum at ca. 190 nm (Figure 10B). Analysis of the $A\beta_{C18C33}$ CD spectra using the secondary structure analysis server BeStSel[72,73] indicates the formation of ca. 50% antiparallel β-sheet structure as the concentration of DDM is raised above the CMC (Figure 10C). In contrast, the $A\beta_{(M1–42)}$ spectra show only ca. 20% antiparallel β-sheet structure under these conditions (Figure 10C). These results further support a model in which the disulfide bond stabilizes a β-hairpin conformation in $A\beta_{C18C33}$ in the membrane-like environments provided by detergents.[52,74]

ThT, TEM, AUC, and DLS Studies of $A\beta_{C18C33}$.

To determine the effect of the disulfide bond upon fibril formation, we performed thioflavin T (ThT) fluorescence assays. Solutions of $A\beta_{C18C33}$ and $A\beta_{(M1–42)}$ were incubated in PBS buffer at pH 7.4 in the presence of ThT at 37 °C. Under these conditions, $A\beta_{(M1–42)}$ showed a characteristic lag time, followed by a rapid onset of fluorescence at ca. 30 minutes (Figure 11B). In contrast, $A\beta_{C18C33}$ showed no appreciable increase in fluorescence over 24 hours (Figure 11A). To rule out the possibility that the $A\beta_{C18C33}$ peptide resists fibrilization because of the cysteine mutations, rather than the intramolecular disulfide bond, we performed a ThT assay using an $A\beta_{C18C33}$ analogue containing two alanine mutations, $A\beta_{A18A33}$. Under comparable conditions, the $A\beta_{A18A33}$ peptide showed a lag time of ca. 4.5 hours, followed by a rapid onset of fluorescence (Figure 11C). These observations demonstrate that the disulfide bond prevents fibril formation. The longer lag time associated with the $A\beta_{A18A33}$ mutant likely reflects the effect of the valine-to-alanine mutation at position 18 of the critical ^{17}LVFFA^{21} amyloidogenic region of Aβ.

We performed transmission electron microscopy (TEM) to corroborate that $A\beta_{C18C33}$ does not fibrilize. Incubation of $A\beta_{C18C33}$ at 37 °C for 24 hours in PBS buffer, followed by TEM imaging, showed no fibrils (Figure 12A). In contrast, $A\beta_{(M1–42)}$ showed long fibrils, typical of Aβ (Figure 12B). $A\beta_{A18A33}$ also showed fibrils, albeit shorter than the characteristic $A\beta_{(M1–42)}$ fibrils (Figure 12C). Upon treatment with TCEP to reduce the disulfide bond and incubation in PBS buffer, $A\beta_{C18C33}$ showed fibrils (Figure 12D). Collectively, these results confirm that the intramolecular disulfide bond is critical to arresting the $A\beta_{C18C33}$ peptide in the oligomeric state.

To further assess the aggregation of the $A\beta_{C18C33}$ peptide in aqueous solution without detergent, we performed analytical ultracentrifugation (AUC) and dynamic light scattering (DLS) experiments. Sedimentation velocity AUC experiments in 10 mM sodium phosphate buffer with 25 mM NaCl at pH 7.4 on samples of $A\beta_{C18C33}$ at 5–160 μM showed a range of oligomeric species up to 70–80 kDa, as well as monomer, with larger oligomeric species becoming more prevalent at higher concentrations (Figure S4). Larger aggregates that settled rapidly were also observed to pellet in these 60,000 rpm experiments and constituted 52–76% of the sample. In DLS experiments, a freshly prepared solution of $A\beta_{C18C33}$ (30 μM in 10 mM sodium phosphate buffer at pH 7.4) showed a peak centered at a hydrodynamic diameter of 24.4 nm (Figure 13). Upon incubation for 24 hours at 37 °C, the peak shifted to 32.7 nm. These results show that $A\beta_{C18C33}$ forms large stable oligomeric assemblies in aqueous solution in the absence of detergent, and are consistent with the pelleting observed in the AUC experiments. Monomer and dimer are likely in equilibrium with these assemblies, but are too small to be observed by DLS. In contrast, a freshly prepared solution of $A\beta_{(M1–42)}$ showed a peak centered at 58.8 nm, which shifted to 955 nm upon incubation for 24 hours (Figure 13). These observations are consistent with the fibril formation observed in the ThT and TEM experiments.

Structure of the $A\beta_{C18C33}$ Dimer.

Thus far, we have not been able to determine the structure of the $A\beta_{C18C33}$ dimer. The ^{1}H NMR spectrum of $A\beta_{C18C33}$ is broad in aqueous solution, and efforts to obtain a ^{1}H–^{15}N HSQC spectrum of ^{15}N-labeled $A\beta_{C18C33}$ in the presence of detergents using simple solution-phase NMR techniques have not been successful. Nevertheless, we believe that the recently published NMR structure of an $A\beta_{42}$ tetramer by Carulla and coworkers (Figure 14A, PDB 6RHY) holds clues into a potential structure of the $A\beta_{C18C33}$ dimer.[58] The tetramer consists of two $A\beta_{42}$ β-hairpins that flank two C-terminal $A\beta_{42}$ β-strands. In each β-hairpin, valine 18 and glycine 33 are proximal and form a non-hydrogen-bonded pair.

In our working model for the $A\beta_{C18C33}$ dimer, the cysteine 18-cysteine 33 disulfide linkage stabilizes this β-hairpin conformation. Two $A\beta_{C18C33}$ β-hairpins hydrogen bond together, without the intervening C-terminal $A\beta_{42}$ β-strands that make up the Carulla tetramer. Figure 14B illustrates this working model for the structure of the $A\beta_{C18C33}$ dimer. An attractive feature of this model is that the C-terminus of each monomer subunit is proximal to the side chain of Lys_{28} in the other monomer subunit, allowing for a salt bridge. We think this model for the dimer of full-length Aβ is reasonable because our laboratory has previously observed similar hydrogen-bonded dimers of other constrained β-hairpin peptides[75–78] and because we have found that the lipophilic environment provided by SDS micelles supports hydrogen-bonding interactions.[79–81]

Conclusion

$A\beta_{C18C33}$, a double mutant of the expressed peptide $A\beta_{(M1–42)}$ containing an intramolecular disulfide bond, forms stable noncovalent dimers in the presence of anionic and non-ionic detergents. The dimers exhibit a high degree of β-sheet character and can readily be observed by SDS-PAGE and mass spectrometry. In aqueous buffer without detergent, the

$A\beta_{C18C33}$ peptide does not aggregate to form fibrils, but instead forms solutions of large oligomers, as well as smaller oligomers and monomer. The membrane-like environment provided by the detergents thus facilitates the formation of dimers. The $A\beta_{C18C33}$ peptide is readily prepared by expression in *E. coli* and can be purified by preparative reverse-phase HPLC. We have deposited the plasmid to express $A\beta_{C18C33}$ at Addgene to make it available to other researchers.[82]

Aβ oligomers continue to be studied intensively through a variety of experimental and computational methods.[83–91] We anticipate that $A\beta_{C18C33}$ will be a valuable tool in biological and biophysical experiments, by providing ready access to stable, homogeneous, noncovalent Aβ dimers. Oligomers of native Aβ peptides ($AB_{1–40}$, $AB_{1–42}$, $A\beta_{(M1–42)}$, etc.) are heterogeneous and prone to further aggregation to form fibrils. Oligomeric preparations of these peptides can thus be problematic to use in biological and biophysical studies. The $A\beta_{C18C33}$ peptide provides an attractive alternative to these preparations, because of the stability and homogeneity of the dimers that it forms in membrane-like environments.

Supplementary Material

Refer to Web version on PubMed Central for supplementary material.

Acknowledgments

This work was supported by the National Institutes of Health (NIH) National Institute of General Medical Sciences (NIGMS) grant GM097562 and National Institute on Aging (NIA) grant AG072587. The authors thank Dr. Dmitry Fishman (UCI Department of Chemistry Laser Spectroscopy Facility), Dr. Philip R. Dennison (UCI Department of Chemistry Nuclear Magnetic Resonance Spectroscopy Facility), and Dr. Li Xing (Irvine Materials Research Institute) for their assistance and discussions. The authors also thank members of the Martin, Tsai, Spitale, and Weiss laboratories for providing helpful advice and access to equipment. High-resolution native mass spectrometry was supported in part by the NIH P41 Resource for Native Mass Spectrometry Guided Structural Biology, P41GM128577 (VHW). Analytical ultracentrifugation experiments were performed at the Canadian Center for Hydrodynamics (CCH) at the University of Lethbridge. The CCH is supported by the Canada 150 Research Chairs program C150-2017-00015 (BD) and the Canada Foundation for Innovation grant CFI-37589 (BD). The UltraScan software development is supported by the National Institutes of Health through grant 1R01GM120600 (BD). Amy Henrickson is supported by the Canadian Natural Science and Engineering Research Council through grant DG-RGPIN-2019-05637 (BD). UltraScan supercomputer calculations were supported through NSF/XSEDE grant TG-MCB070039N (B.D), and University of Texas grant TG457201 (B.D). Computational resources and support from the University of Montana's Griz Shared Computing Cluster (GSCC) contributed to this research.

References and notes

(1). Narayan P; Ganzinger KA; McColl J; Weimann L; Meehan S; Qamar S; Carver JA; Wilson MR; St. George-Hyslop P; Dobson CM; Klenerman D Single Molecule Characterization of the Interactions between Amyloid-β Peptides and the Membranes of Hippocampal Cells. J. Am. Chem. Soc 2013, 135 (4), 1491–1498. 10.1021/ja3103567. [PubMed: 23339742]

(2). Evangelisti E; Cascella R; Becatti M; Marrazza G; Dobson CM; Chiti F; Stefani M; Cecchi C Binding Affinity of Amyloid Oligomers to Cellular Membranes Is a Generic Indicator of Cellular Dysfunction in Protein Misfolding Diseases. Sci. Rep 2016, 6, 32721. 10.1038/srep32721. [PubMed: 27619987]

(3). Haass C; Selkoe DJ Soluble Protein Oligomers in Neurodegeneration: Lessons from the Alzheimer's Amyloid β-Peptide. Nat. Rev. Mol. Cell Biol 2007, 8, 101–112. 10.1038/nrm2101. [PubMed: 17245412]

(4). Ferreira ST; Lourenco MV; Oliveira MM; De Felice FG Soluble Amyloid-β Oligomers as Synaptotoxins Leading to Cognitive Impairment in Alzheimer's Disease. Front. Cell. Neurosci 2015, 9, 191. 10.3389/fncel.2015.00191. [PubMed: 26074767]

(5). Benilova I; Karran E; De Strooper B The Toxic Aβ Oligomer and Alzheimer's Disease: An Emperor in Need of Clothes. Nat. Neurosci 2012, 15, 349–357. 10.1038/nn.3028. [PubMed: 22286176]

(6). Selkoe DJ; Hardy J The Amyloid Hypothesis of Alzheimer's Disease at 25 Years. EMBO Mol. Med 2016, 8 (6), 595–608. 10.15252/emmm.201606210. [PubMed: 27025652]

(7). Yang T; Li S; Xu H; Walsh DM; Selkoe DJ Large Soluble Oligomers of Amyloid β-Protein from Alzheimer Brain Are Far Less Neuroactive than the Smaller Oligomers to Which They Dissociate. J. Neurosci 2017, 37 (1), 152–163. 10.1523/JNEUROSCT.1698-16.2016. [PubMed: 28053038]

(8). Cizas P; Budvytyte R; Morkuniene R; Moldovan R; Broccio M; Lösche M; Niaura G; Valincius G; Borutaite V Size-Dependent Neurotoxicity of β-Amyloid Oligomers. Arch. Biochem. Biophys 2010, 496 (2), 84–92. 10.1016/j.abb.2010.02.001. [PubMed: 20153288]

(9). Ono K; Condron MM; Teplow DB Structure-Neurotoxicity Relationships of Amyloid β-Protein Oligomers. Proc. Natl. Acad. Sci. U. S. A 2009, 106 (35), 14745–14750. 10.1073/pnas.0905127106. [PubMed: 19706468]

(10). Man VH; Nguyen PH; Derreumaux P High-Resolution Structures of the Amyloid-β 1-42 Dimers from the Comparison of Four Atomistic Force Fields. J. Phys. Chem. B 2017, 121 (24), 5977–5987. 10.1021/acs.jpcb.7b04689. [PubMed: 28538095]

(11). Vázquez De La Torre A; Gay M; Vilaprinyó-Pascual S; Mazzucato R; Serra-Batiste M; Vilaseca M; Carulla N Direct Evidence of the Presence of Cross-Linked Aβ Dimers in the Brains of Alzheimer's Disease Patients. Anal. Chem 2018, 90 (7), 4552–4560. 10.1021/acs.analchem.7b04936. [PubMed: 29537826]

(12). Brinkmalm G; Hong W; Wang Z; Liu W; O'Malley TT; Sun X; Frosch MP; Selkoe DJ; Portelius E; Zetterberg H; Blennow K; Walsh DM Identification of Neurotoxic Cross-Linked Amyloid-β Dimers in the Alzheimer's Brain. Brain 2019, 142 (5), 1441–1457. 10.1093/brain/awz066. [PubMed: 31032851]

(13). Jin M; Shepardson N; Yang T; Chen G; Walsh D; Selkoe DJ Soluble Amyloid β-Protein Dimers Isolated from Alzheimer Cortex Directly Induce Tau Hyperphosphorylation and Neuritic Degeneration. Proc. Natl. Acad. Sci. U. S. A 2011, 108 (14), 5819–5824. 10.1073/pnas.1017033108. [PubMed: 21421841]

(14). Klyubin I; Betts V; Welzel AT; Blennow K; Zetterberg H; Wallin A; Lemere CA; Cullen WK; Peng Y; Wisniewski T; Selkoe DJ; Anwyl R; Walsh DM; Rowan MJ Amyloid β Protein Dimer-Containing Human CSF Disrupts Synaptic Plasticity: Prevention by Systemic Passive Immunization. J. Neurosci 2008, 28 (16), 4231–4237. 10.1523/JNEUROSCI.5161-07.2008. [PubMed: 18417702]

(15). Shankar GM; Li S; Mehta TH; Garcia-Munoz A; Shepardson NE; Smith I; Brett FM; Farrell MA; Rowan MJ; Lemere CA; Regan CM; Walsh DM; Sabatini BL; Selkoe DJ Amyloid-β Protein Dimers Isolated Directly from Alzheimer's Brains Impair Synaptic Plasticity and Memory. Nat. Med 2008, 14 (8), 837–842. 10.1038/nm1782. [PubMed: 18568035]

(16). O'Nuallain B; Freir DB; Nicoll AJ; Risse E; Ferguson N; Herron CE; Collinge J; Walsh DM Amyloid β-Protein Dimers Rapidly Form Stable Synaptotoxic Protofibrils. J. Neurosci 2010, 30 (43), 14411–14419. 10.1523/JNEUROSCI.3537-10.2010. [PubMed: 20980598]

(17). Abdel-Hafiz L; Müller-Schiffmann A; Korth C; Fazari B; Chao OY; Nikolaus S; Schäble S; Herring A; Keyvani K; Lamounier-Zepter V; Huston JP; de Souza Silva MA Aβ Dimers Induce Behavioral and Neurochemical Deficits of Relevance to Early Alzheimer's Disease. Neurobiol. Aging 2018, 69, 1–9. 10.1016/j.neurobiolaging.2018.04.005. [PubMed: 29803148]

(18). Müller-Schiffmann A; Herring A; Abdel-Hafiz L; Chepkova AN; Schäble S; Wedel D; Horn AHC; Sticht H; De Souza Silva MA; Gottmann K; Sergeeva OA; Huston JP; Keyvani K; Korth C Amyloid-β Dimers in the Absence of Plaque Pathology Impair Learning and Synaptic Plasticity. Brain 2016, 139 (2), 509–525. 10.1093/brain/awv355. [PubMed: 26657517]

(19). Hirel PH; Schmitter JM; Dessen P; Fayat G; Blanquet S Extent of N-Terminal Methionine Excision from Escherichia Coli Proteins Is Governed by the Side-Chain Length of the Penultimate Amino Acid. Proc. Natl. Acad. Sci. U. S. A 1989, 86 (21), 8247–8251. 10.1073/pnas.86.21.8247. [PubMed: 2682640]

(20). Salveson PJ; Spencer RK; Kreutzer AG; Nowick JS X-Ray Crystallographic Structure of a Compact Dodecamer from a Peptide Derived from Aβ16-36. Org. Lett 2017, 19 (13), 3462–3465. 10.1021/acs.orglett.7b01445. [PubMed: 28683555]

(21). Cline EN; Bicca MA; Viola KL; Klein WL The Amyloid-β Oligomer Hypothesis: Beginning of the Third Decade. J. Alzheimer's Dis 2018, 64, S567–S610. 10.3233/JAD-179941. [PubMed: 29843241]

(22). Orte A; Birkett NR; Clarke RW; Devlin GL; Dobson CM; Klenerman D Direct Characterization of Amyloidogenic Oligomers by Single-Molecule Fluorescence. Proc. Natl. Acad. Sci. U. S. A 2008, 105 (38), 14424–14429. 10.1073/pnas.0803086105. [PubMed: 18796612]

(23). Marina GB; Kirkitadze D; Lomakin A; Vollers SS; Benedek GB; Teplow DB Amyloid β-Protein (AB) Assembly: Aβ40 and Aβ42 Oligomerize through Distinct Pathways. Proc. Natl. Acad. Sci. U. S. A 2003, 100 (1), 330–335. 10.1073/pnas.222681699. [PubMed: 12506200]

(24). Bitan G; Lomakin A; Teplow DB Amyloid β-Protein Oligomerization: Prenucleation Interactions Revealed by Photo-Induced Cross-Linking of Unmodified Proteins. J. Biol. Chem 2001, 276 (37), 35176–35184. 10.1074/jbc.M102223200. [PubMed: 11441003]

(25). Chen GF; Xu TH; Yan Y; Zhou YR; Jiang Y; Melcher K; Xu HE Amyloid Beta: Structure, Biology and Structure-Based Therapeutic Development. Acta Pharmacol. Sin 2017, 38, 1205–1235. 10.1038/aps.2017.28. [PubMed: 28713158]

(26). Knowles TPJ; Vendruscolo M; Dobson CM The Amyloid State and Its Association with Protein Misfolding Diseases. Nat. Rev. Mol. Cell Biol 2014, 15, 384–396. 10.1038/nrm3810. [PubMed: 24854788]

(27). Makin OS; Atkins E; Sikorski P; Johansson J; Serpell LC Molecular Basis for Amyloid Fibril Formation and Stability. Proc. Natl. Acad. Sci. U. S. A 2005, 102 (2), 315–320. 10.1073/pnas.0406847102. [PubMed: 15630094]

(28). OMalley TT; Walsh DM Lessons from the Study of Covalent Dimers of the Alzheimer's Disease-Associate Amyloid β-Protein. Biochem. Physiol. Open Access 2018, 07 (01), 229. 10.4172/2168-9652.1000229.

(29). Ryan DA; Narrow WC; Federoff HJ; Bowers WJ An Improved Method for Generating Consistent Soluble Amyloid-Beta Oligomer Preparations for in Vitro Neurotoxicity Studies. J. Neurosci. Methods 2010, 190 (2), 171–179. 10.1016/j.jneumeth.2010.05.001. [PubMed: 20452375]

(30). Pitt J; Roth W; Lacor P; Smith AB; Blankenship M; Velasco P; De Felice F; Breslin P; Klein WL Alzheimer's-Associated Aβ Oligomers Show Altered Structure, Immunoreactivity and Synaptotoxicity with Low Doses of Oleocanthal. Toxicol. Appl. Pharmacol 2009, 240 (2), 189–197. 10.1016/j.taap.2009.07.018. [PubMed: 19631677]

(31). O'Malley TT; Witbold WM; Linse S; Walsh DM The Aggregation Paths and Products of Aβ42 Dimers Are Distinct from Those of the Aβ42 Monomer. Biochemistry 2016, 55 (44), 6150–6161. 10.1021/acs.biochem.6b00453. [PubMed: 27750419]

(32). Hartley DM; Zhao C; Speier AC; Woodard GA; Li S; Li Z; Walz T Transglutaminase Induces Protofibril-like Amyloid β-Protein Assemblies That Are Protease-Resistant and Inhibit Long-Term Potentiation. J. Biol. Chem 2008, 283 (24), 16790–16800. 10.1074/jbc.M802215200. [PubMed: 18397883]

(33). Sitkiewicz E; Olędzki J; Poznański J; Dadlez M Di-Tyrosine Cross-Link Decreases the Collisional Cross-Section of Aβ Peptide Dimers and Trimers in the Gas Phase: An Ion Mobility Study. PLoS One 2014, 9 (6), e100200. 10.1371/journal.pone.0100200. [PubMed: 24945725]

(34). O'Malley TT; Oktaviani NA; Zhang D; Lomakin A; O'Nuallain B; Linse S; Benedek GB; Rowan MJ; Mulder FAA; Walsh DM Aβ Dimers Differ from Monomers in Structural Propensity, Aggregation Paths and Population of Synaptotoxic Assemblies. Biochem. J 2014, 461 (3), 413–426. 10.1042/BJ20140219. [PubMed: 24785004]

(35). Atwood CS; Perry G; Zeng H; Kato Y; Jones WD; Ling KQ; Huang X; Moir RD; Wang D; Sayre LM; Smith MA; Chen SG; Bush AI Copper Mediates Dityrosine Cross-Linking of Alzheimer's Amyloid-β. Biochemistry 2004, 43 (2), 560–568. 10.1021/bi0358824. [PubMed: 14717612]

(36). Yamaguchi T; Yagi H; Goto Y; Matsuzaki K; Hoshino M A Disulfide-Linked Amyloid-β Peptide Dimer Forms a Protofibril-like Oligomer through a Distinct Pathway from Amyloid Fibril Formation. Biochemistry 2010, 49 (33), 7100–7107. 10.1021/bi100583x. [PubMed: 20666485]

(37). Müller-Schiffmann A; Andreyeva A; Horn AHC; Gottmann K; Korth C; Sticht H Molecular Engineering of a Secreted, Highly Homogeneous, and Neurotoxic Aβ Dimer. ACS Chem. Neurosci 2011, 2 (5), 242–248. 10.1021/cn200011h. [PubMed: 22778868]

(38). Murakami K; Kato H; Hanaki M; Monobe Y; Akagi KI; Kawase T; Hirose K; Irie K Synthetic and Biochemical Studies on the Effect of Persulfidation on Disulfide Dimer Models of Amyloid SS42 at Position 35 in Alzheimer's Etiology. RSC Adv. 2020, 10 (33), 19506–19512. 10.1039/d0ra03429k. [PubMed: 35515472]

(39). Schützmann MP; Hasecke F; Bachmann S; Zielinski M; Hänsch S; Schröder GF; Zempel H; Hoyer W Endo-Lysosomal Aβ Concentration and PH Trigger Formation of Aβ Oligomers That Potently Induce Tau Missorting. Nat. Commun 2021, 12 (1), 1–14. 10.1038/s41467-021-24900-4. [PubMed: 33397941]

(40). Hasecke F; Miti T; Perez C; Barton J; Schölzel D; Gremer L; Grüning CSR; Matthews G; Meisl G; Knowles TPJ; Willbold D; Neudecker P; Heise H; Ullah G; Hoyer W; Muschol M Origin of Metastable Oligomers and Their Effects on Amyloid Fibril Self-Assembly. Chem. Sci 2018, 9 (27), 5937–5948. 10.1039/C8SC01479E. [PubMed: 30079208]

(41). Murakami K; Suzuki T; Hanaki M; Monobe Y; Akagi KI; Irie K Synthesis and Characterization of the Amyloid B40 Dimer Model with a Linker at Position 30 Adjacent to the Intermolecular β-Sheet Region. Biochem. Biophys. Res. Commun 2015, 466 (3), 463–467. 10.1016/j.bbrc.2015.09.051. [PubMed: 26367176]

(42). Kok WM; Scanlon DB; Karas JA; Miles LA; Tew DJ; Parker MW; Barnham KJ; Hutton CA Solid-Phase Synthesis of Homodimeric Peptides: Preparation of Covalently-Linked Dimers of Amyloid β Peptide. Chem. Commun 2009, No. 41, 6228–6230. 10.1039/b912784d.

(43). Murakami K; Tokuda M; Suzuki T; Irie Y; Hanaki M; Izuo N; Monobe Y; Akagi KI; Ishii R; Tatebe H; Tokuda T; Maeda M; Kume T; Shimizu T; Irie K Monoclonal Antibody with Conformational Specificity for a Toxic Conformer of Amyloid B42 and Its Application toward the Alzheimer's Disease Diagnosis. Sci. Rep 2016, 6, 29038. 10.1038/srep29038. [PubMed: 27374357]

(44). Siegel SJ; Bieschke J; Powers ET; Kelly JW The Oxidative Stress Metabolite 4-Hydroxynonenal Promotes Alzheimer Protofibril Formation. Biochemistry 2007, 46 (6), 1503–1510. 10.1021/bi061853s. [PubMed: 17279615]

(45). Hayden EY; Conovaloff JL; Mason A; Bitan G; Teplow DB Preparation of Pure Populations of Amyloid β-Protein Oligomers of Defined Size. Methods Mol. Biol 2018, 1779, 3–12. 10.1007/978-1-4939-7816-8_1. [PubMed: 29886523]

(46). Rosensweig C; Ono K; Murakami K; Lowenstein DK; Bitan G; Teplow DB Preparation of Stable Amyloid β-Protein Oligomers of Defined Assembly Order. Methods Mol. Biol 2012, 849, 23–31. 10.1007/978-1-61779-551-0_3. [PubMed: 22528081]

(47). Hayden EY; Conovaloff JL; Mason A; Bitan G; Teplow DB Preparation of Pure Populations of Covalently Stabilized Amyloid β-Protein Oligomers of Specific Sizes. Anal. Biochem 2017, 518, 78–85. 10.1016/j.ab.2016.10.026. [PubMed: 27810329]

(48). Nag S; Sarkar B; Bandyopadhyay A; Sahoo B; Sreenivasan VKA; Kombrabail M; Muralidharan C; Maiti S Nature of the Amyloid-β Monomer and the Monomer-Oligomer Equilibrium. J. Biol. Chem 2011, 286 (16), 13827–13833. 10.1074/jbc.M110.199885. [PubMed: 21349839]

(49). Soreghan B; Kosmoski J; Glabe C Surfactant Properties of Alzheimer's Aβ Peptides and the Mechanism of Amyloid Aggregation. J. Biol. Chem 1994, 269 (46), 28551–28554. [PubMed: 7961799]

(50). Dear AJ; Michaels TCT; Meisl G; Klenerman D; Wu S; Perrett S; Linse S; Dobson CM; Knowles TPJ Kinetic Diversity of Amyloid Oligomers. Proc. Natl. Acad. Sci. U. S. A 2020, 117 (22), 12087–12094. 10.1073/pnas.1922267117. [PubMed: 32414930]

(51). Dubnovitsky A; Sandberg A; Rahman MM; Benilova I; Lendel C; Härd T Amyloid-β Protofibrils: Size, Morphology and Synaptotoxicity of an Engineered Mimic. PLoS One 2013, 8 (7), e66101. 10.1371/journal.pone.0066101. [PubMed: 23843949]

(52). Sandberg A; Luheshi LM; Söllvander S; De Barros TP; Macao B; Knowles TPJ; Biverstål H; Lendel C; Ekholm-Petterson F; Dubnovitsky A; Lannfelt L; Dobson CM; Härd T Stabilization of Neurotoxic Alzheimer Amyloid-β Oligomers by Protein Engineering. Proc. Natl. Acad. Sci. U. S. A 2010, 107 (35), 15595–15600. 10.1073/pnas.1001740107. [PubMed: 20713699]

(53). Lendel C; Bjerring M; Dubnovitsky A; Kelly RT; Filippov A; Antzutkin ON; Nielsen NC; Härd T A Hexameric Peptide Barrel as Building Block of Amyloid-β Protofibrils. Angew. Chemie - Int. Ed 2014, 53 (47), 12756–12760. 10.1002/anie.201406357.

(54). Hoyer W; Grönwall C; Jonsson A; Ståhl S; Härd T Stabilization of a β-Hairpin in Monomeric Alzheimer's Amyloid-β Peptide Inhibits Amyloid Formation. Proc. Natl. Acad. Sci. U. S. A 2008, 105 (13), 5099–5104. 10.1073/pnas.0711731105. [PubMed: 18375754]

(55). Matsushima Y; Yanagita RC; Irie K Control of the Toxic Conformation of Amyloid B42 by Intramolecular Disulfide Bond Formation. Chem. Commun 2020, 56 (29), 4118–4121. 10.1039/d0cc01053g.

(56). Yamamoto M; Shinoda K; Ni J; Sasaki D; Kanai M; Sohma Y A Chemically Engineered, Stable Oligomer Mimic of Amyloid B42 Containing an Oxime Switch for Fibril Formation. Org. Biomol. Chem 2018, 16 (35), 6537–6542. 10.1039/c8ob01875h. [PubMed: 30167602]

(57). Yu L; Edalji R; Harlan JE; Holzman TF; Lopez AP; Labkovsky B; Hillen H; Barghorn S; Ebert U; Richardson PL; Miesbauer L; Solomon L; Bartley D; Walter K; Johnson RW; Hajduk PJ; Olejniczak ET Structural Characterization of a Soluble Amyloid β-Peptide Oligomer. Biochemistry 2009, 48 (9), 1870–1877. 10.1021/bi802046n. [PubMed: 19216516]

(58). Ciudad S; Puig E; Botzanowski T; Meigooni M; Arango AS; Do J; Mayzel M; Bayoumi M; Chaignepain S; Maglia G; Cianferani S; Orekhov V; Tajkhorshid E; Bardiaux B; Carulla N Aβ(1-42) Tetramer and Octamer Structures Reveal Edge Conductivity Pores as a Mechanism for Membrane Damage. Nat. Commun 2020, 11 (1), 3014. 10.1038/s41467-020-16566-1. [PubMed: 32541820]

(59). Ghosh U; Thurber KR; Yau W-M; Tycko R Molecular Structure of a Prevalent Amyloid-β Fibril Polymorph from Alzheimer's Disease Brain Tissue. Proc. Natl. Acad. Sci. U. S. A 2021, 118 (4), e2023089118. 10.1073/PNAS.2023089118. [PubMed: 33431654]

(60). For studies of artificial oligomers formed by Aβ fragments, see the following, as well as citations 60–63:Samdin TD; Kreutzer AG; Nowick JS Exploring Amyloid Oligomers with Peptide Model Systems. Curr. Opin. Chem. Biol 2021, 64, 106–115. 10.1016/J.CBPA.2021.05.004. [PubMed: 34229162]

(61). Samdin TD; Wierzbicki M; Kreutzer AG; Howitz WJ; Valenzuela M; Smith A; Sahrai V; Truex NL; Klun M; Nowick JS Effects of N-Terminal Residues on the Assembly of Constrained β-Hairpin Peptides Derived from Aβ. J. Am. Chem. Soc 2020, 142 (26), 11593–11601. 10.1021/JACS.0C05186. [PubMed: 32501687]

(62). Kreutzer AG; Yoo S; Spencer RK; Nowick JS Stabilization, Assembly, and Toxicity of Trimers Derived from Aβ. J. Am. Chem. Soc 2017, 139 (2), 966–975. 10.1021/jacs.6b11748. [PubMed: 28001392]

(63). Kreutzer AG; Hamza IL; Spencer RK; Nowick JS X-Ray Crystallographic Structures of a Trimer, Dodecamer, and Annular Pore Formed by an Aβ17-36 β-Hairpin. J. Am. Chem. Soc 2016, 138 (13), 4634–4642. 10.1021/JACS.6B01332. [PubMed: 26967810]

(64). Spencer RK; Li H; Nowick JS X-Ray Crystallographic Structures of Trimers and Higher-Order Oligomeric Assemblies of a Peptide Derived from Aβ17-36. J. Am. Chem. Soc 2014, 136 (15), 5595–5598. 10.1021/ja5017409. [PubMed: 24669800]

(65). Yoo S; Zhang S; Kreutzer AG; Nowick JS An Efficient Method for the Expression and Purification of Aβ(M1-42). Biochemistry 2018, 57 (26), 3861–3866. 10.1021/acs.biochem.8b00393. [PubMed: 29757632]

(66). Zhang S; Guaglianone G; Morris MA; Yoo S; Howitz WJ; Xing L; Zheng JG; Jusuf H; Huizar G; Lin J; Kreutzer AG; Nowick JS Expression of N-Terminal Cysteine Aβ42and Conjugation to Generate Fluorescent and Biotinylated Aβ42. Biochemistry 2021, 60 (15), 1191–1200. 10.1021/ACS.BIOCHEM.1C00105. [PubMed: 33793198]

(67). Salveson PJ; Spencer RK; Kreutzer AG; Nowick JS X-Ray Crystallographic Structure of a Compact Dodecamer from a Peptide Derived from Aβ16-36. Org. Lett 2017, 19 (13), 3462–3465. 10.1021/acs.orglett.7b01445. [PubMed: 28683555]

(68). Silvers R; Colvin MT; Frederick KK; Jacavone AC; Lindquist S; Linse S; Griffin RG Aggregation and Fibril Structure of AβM01-42 and Aβ1-42. Biochemistry 2017, 56 (36), 4850–4859. 10.1021/acs.biochem.7b00729. [PubMed: 28792214]

(69). Kreutzer AG; Samdin TD; Guaglianone G; Spencer RK; Nowick JS X-Ray Crystallography Reveals Parallel and Antiparallel β-Sheet Dimers of a β-Hairpin Derived from Aβ16-36 that Assemble to Form Different Tetramers. ACS Chem. Neurosci 2020, 11 (15), 2340–2347. 10.1021/acschemneuro.0c00290. [PubMed: 32584538]

(70). Pujol-Pina R; Vilaprinyó-Pascual S; Mazzucato R; Arcella A; Vilaseca M; Orozco M; Carulla N SDS-PAGE Analysis of Aβ Oligomers Is Disserving Research into Alzheimer's Disease: Appealing for ESI-IM-MS. Sci. Rep 2015, 5, 14809. 10.1038/srep14809. [PubMed: 26450154]

(71). Olsen JV; Macek B; Lange O; Makarov A; Horning S; Mann M Higher-Energy C-Trap Dissociation for Peptide Modification Analysis. Nat. Methods 2007 49 2007, 4 (9), 709–712. 10.1038/nmeth1060.

(72). Micsonai A; Wien F; Kernya L; Lee YH; Goto Y; Réfrégiers M; Kardos J Accurate Secondary Structure Prediction and Fold Recognition for Circular Dichroism Spectroscopy. Proc. Natl. Acad. Sci. U. S. A 2015, 112 (24), E3095–E3103. 10.1073/pnas.1500851112. [PubMed: 26038575]

(73). Micsonai A; Wien F; Bulyáki É; Kun J; Moussong É; Lee YH; Goto Y; Réfrégiers M; Kardos J BeStSel: A Web Server for Accurate Protein Secondary Structure Prediction and Fold Recognition from the Circular Dichroism Spectra. Nucleic Acids Res. 2018, 46 (W1), W315–W312. 10.1093/nar/gky497. [PubMed: 29893907]

(74). Cerf E; Sarroukh R; Tamamizu-Kato S; Breydo L; Derclayes S; Dufrênes YF; Narayanaswami V; Goormaghtigh E; Ruysschaert JM; Raussens V Antiparallel β-Sheet: A Signature Structure of the Oligomeric Amyloid β-Peptide. Biochem. J 2009, 421 (3), 415–423. 10.1042/BJ20090379. [PubMed: 19435461]

(75). Pham JD; Demeler B; Nowick JS Polymorphism of Oligomers of a Peptide from β-Amyloid. J. Am. Chem. Soc 2014, 136 (14), 5432–5442. 10.1021/ja500996d. [PubMed: 24669785]

(76). Khakshoor O; Lin AJ; Korman TP; Sawaya MR; Tsai SC; Eisenberg D; Nowick JS X-Ray Crystallographic Structure of an Artificial β-Sheet Dimer. J. Am. Chem. Soc 2010, 132 (33), 11622–11628. 10.1021/ja103438w. [PubMed: 20669960]

(77). Khakshoor O; Demeler B; Nowick JS Macrocyclic β-Sheet Peptides That Mimic Protein Quaternary Structure through Intermolecular β-Sheet Interactions. J. Am. Chem. Soc 2007, 129 (17), 5558–5569. 10.1021/ja068511u. [PubMed: 17419629]

(78). Nowick JS; Tsai JH; Bui QD; Maitra S A Chemical Model of a Protein β-Sheet Dimer. J. Am. Chem. Soc 1999, 121 (36), 8409–8410. 10.1021/ja992109g.

(79). Nowick JS; Cao T; Noronha G Molecular Recognition between Uncharged Molecules in Aqueous Micelles. J. Am. Chem. Soc 1994, 116 (8), 3285–3289. 10.1021/ja00087a014. [PubMed: 25084234]

(80). Nowick JS; Chen JS; Noronha G Molecular Recognition in Micelles: The Roles of Hydrogen Bonding and Hydrophobicity in Adenine-Thymine Base-Pairing in SDS Micelles. J. Am. Chem. Soc 1993, 115 (17), 7636–7644. 10.1021/ja00070a007.

(81). Nowick JS; Chen JS Molecular Recognition in Aqueous Micellar Solution: Adenine-Thymine Base-Pairing in SDS Micelles. J. Am. Chem. Soc 1992, 114 (3), 1107–1108. 10.1021/ja00029a060.

(82). Addgene, pET-Sac-Aβ(M1-42/C18C33), Plasmid #173759. https://www.addgene.org/173759/

(83). Nguyen PH; Ramamoorthy A; Sahoo BR; Zheng J; Faller P; Straub JE; Dominguez L; Shea JE; Dokholyan NV; de Simone A; Ma B; Nussinov R; Najafi S; Ngo ST; Loquet A; Chiricotto M; Ganguly P; McCarty J; Li MS; Hall C; Wang Y; Miller Y; Melchionna S; Habenstein B; Timr S; Chen J; Hnath B; Strodel B; Kayed R; Lesné S; Wei G; Sterpone F; Doig AJ; Derreumaux P Amyloid Oligomers: A Joint Experimental/Computational Perspective on Alzheimer's Disease, Parkinson's Disease, Type II Diabetes, and Amyotrophic Lateral Sclerosis. Chem. Rev 2021, 121 (4), 2545–2647. 10.1021/ACS.CHEMREV.0C01122. [PubMed: 33543942]

(84). Kirkitadze MD; Condron MM; Teplow DB Identification and Characterization of Key Kinetic Intermediates in Amyloid Beta-Protein Fibrillogenesis. J. Mol. Biol 2001, 312 (5), 1103–1119. 10.1006/JMBI.2001.4970. [PubMed: 11580253]

(85). Vivekanandan S; Brender JR; Lee SY; Ramamoorthy A A Partially Folded Structure of Amyloid-Beta(1-40) in an Aqueous Environment. Biochem. Biophys. Res. Commun 2011, 411 (2), 312–316. 10.1016/J.BBRC.2011.06.133. [PubMed: 21726530]

(86). Chen M; Schafer NP; Wolynes PG Surveying the Energy Landscapes of Aβ Fibril Polymorphism. J. Phys. Chem. B 2018, 122 (49), 11414–11430. 10.1021/ACS.JPCB.8B07364/SUPPL_FILE/JP8B07364_SI_002.ZIP. [PubMed: 30215519]

(87). Ahmed M; Davis J; Aucoin D; Sato T; Ahuja S; Aimoto S; Elliott JI; Van Nostrand WE; Smith SO Structural Conversion of Neurotoxic Amyloid-Beta(1-42) Oligomers to Fibrils. Nat. Struct. Mol. Biol 2010, 17 (5), 561–567. 10.1038/NSMB.1799. [PubMed: 20383142]

(88). Kotler SA; Brender JR; Vivekanandan S; Suzuki Y; Yamamoto K; Monette M; Krishnamoorthy J; Walsh P; Cauble M; Holl MMB; Marsh ENG; Ramamoorthy A High-Resolution NMR Characterization of Low Abundance Oligomers of Amyloid-β without Purification. Sci. Rep 2015, 5 (1), 1–12. 10.1038/srep11811.

(89). Lopez Del Amo JM; Fink U; Dasari M; Grelle G; Wanker EE; Bieschke J; Reif B Structural Properties of EGCG-Induced, Nontoxic Alzheimer's Disease Aβ Oligomers. J. Mof. Biol 2012, 421 (4–5), 517–524. 10.1016/J.JMB.2012.01.013.

(90). Cawood EE; Karamanos TK; Wilson AJ; Radford SE Visualizing and Trapping Transient Oligomers in Amyloid Assembly Pathways. Biophys. Chem 2021, 268, 106505. 10.1016/J.BPC.2020.106505. [PubMed: 33220582]

(91). Sharma S; Modi P; Sharma G; Deep S Kinetics Theories to Understand the Mechanism of Aggregation of a Protein and to Design Strategies for Its Inhibition. Biophys. Chem 2021, 278, 106665. 10.1016/J.BPC.2021.106665. [PubMed: 34419715]

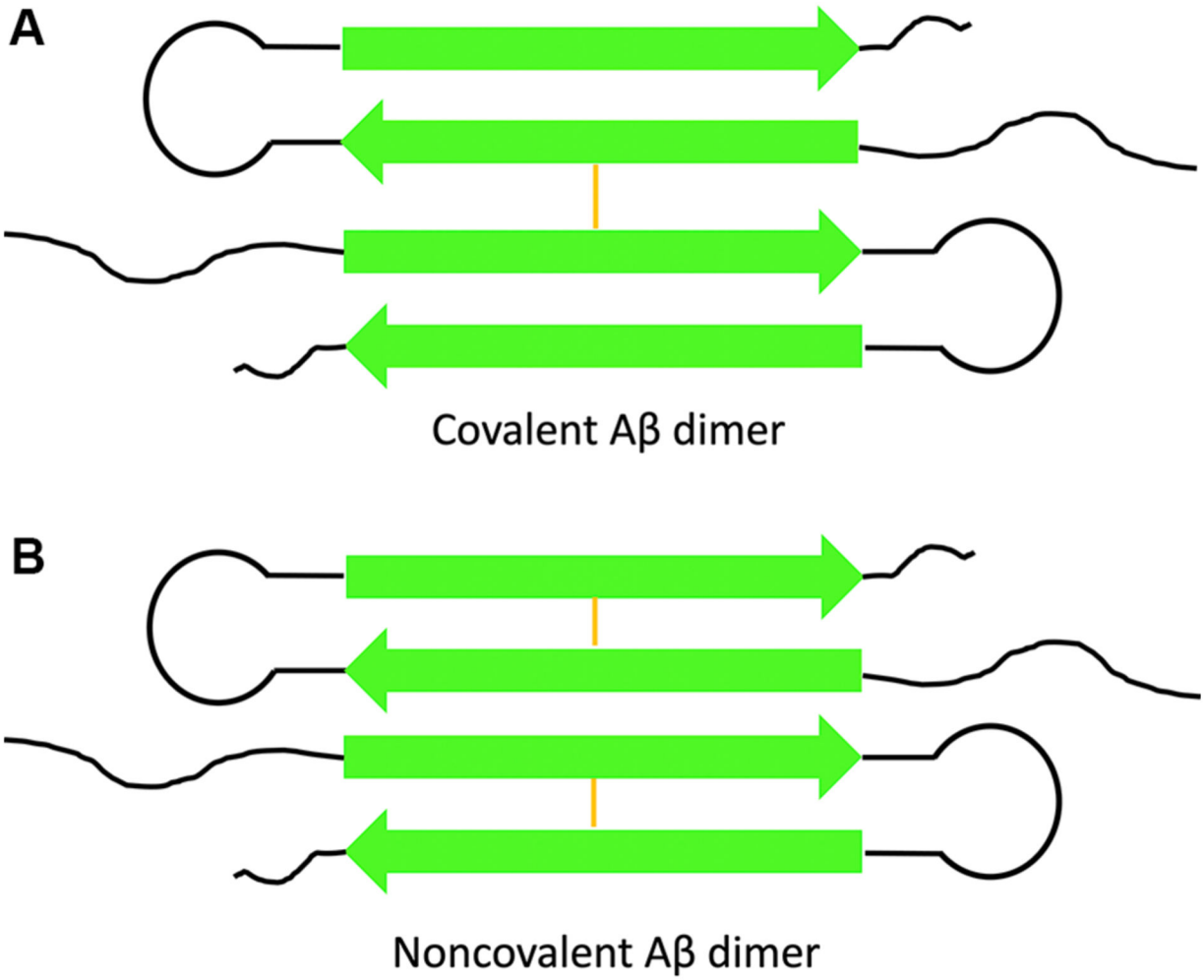

Figure 1.

Cartoons of dimers of Aβ β-hairpins illustrating the differences between covalent and noncovalent dimers. (A) A covalent Aβ dimer generated by an intermolecular disulfide bond. (B) A noncovalent Aβ dimer containing two Aβ monomers stabilized by intramolecular disulfide bonds. Disulfide bonds are shown in solid orange lines.

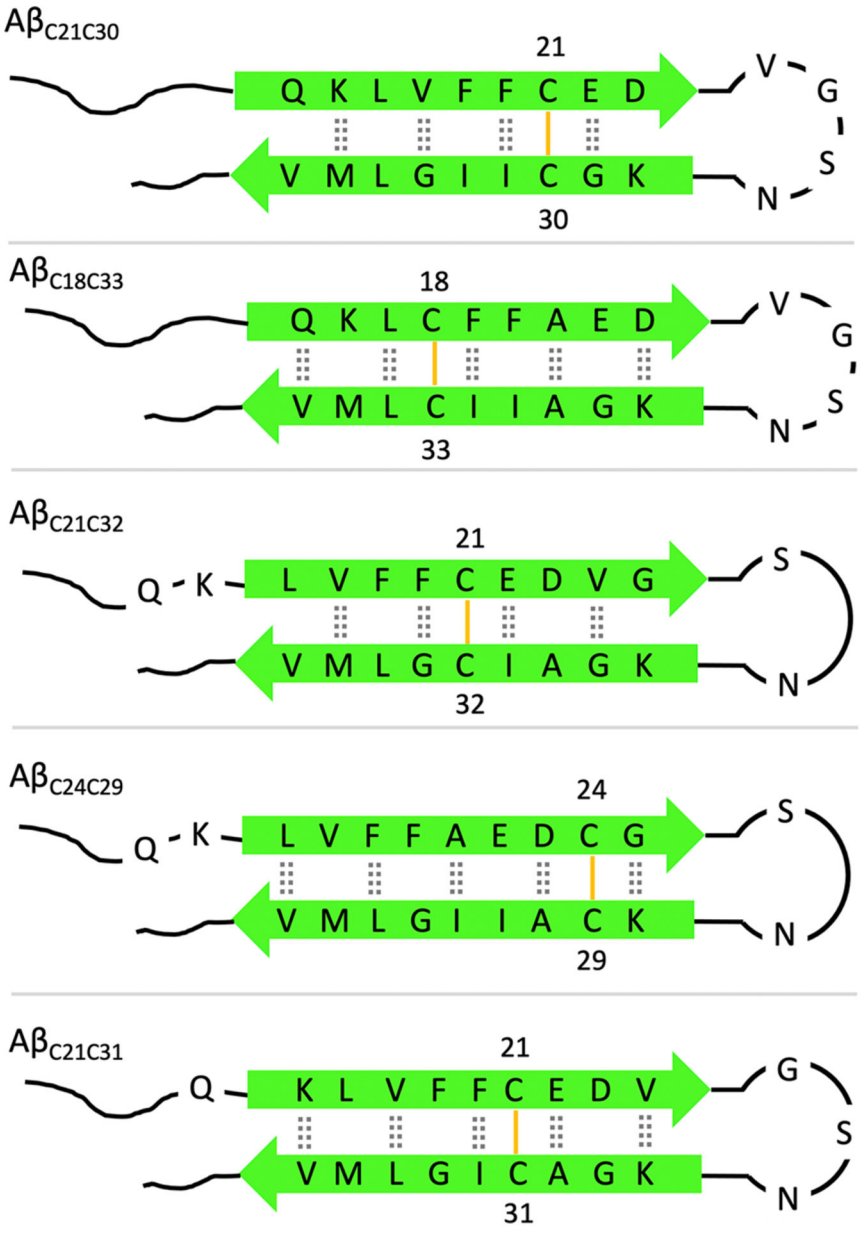

Figure 2.

Cartoons of mutant $A\beta_{42}$ peptides containing intramolecular disulfide bonds that stabilize the peptides in a β-hairpin conformation. Cartoons illustrate β-hairpin structures with different disulfide linkages and residue pairings. Disulfide bonds are shown in solid orange lines. Hydrogen bonds are shown in grey dashed lines.

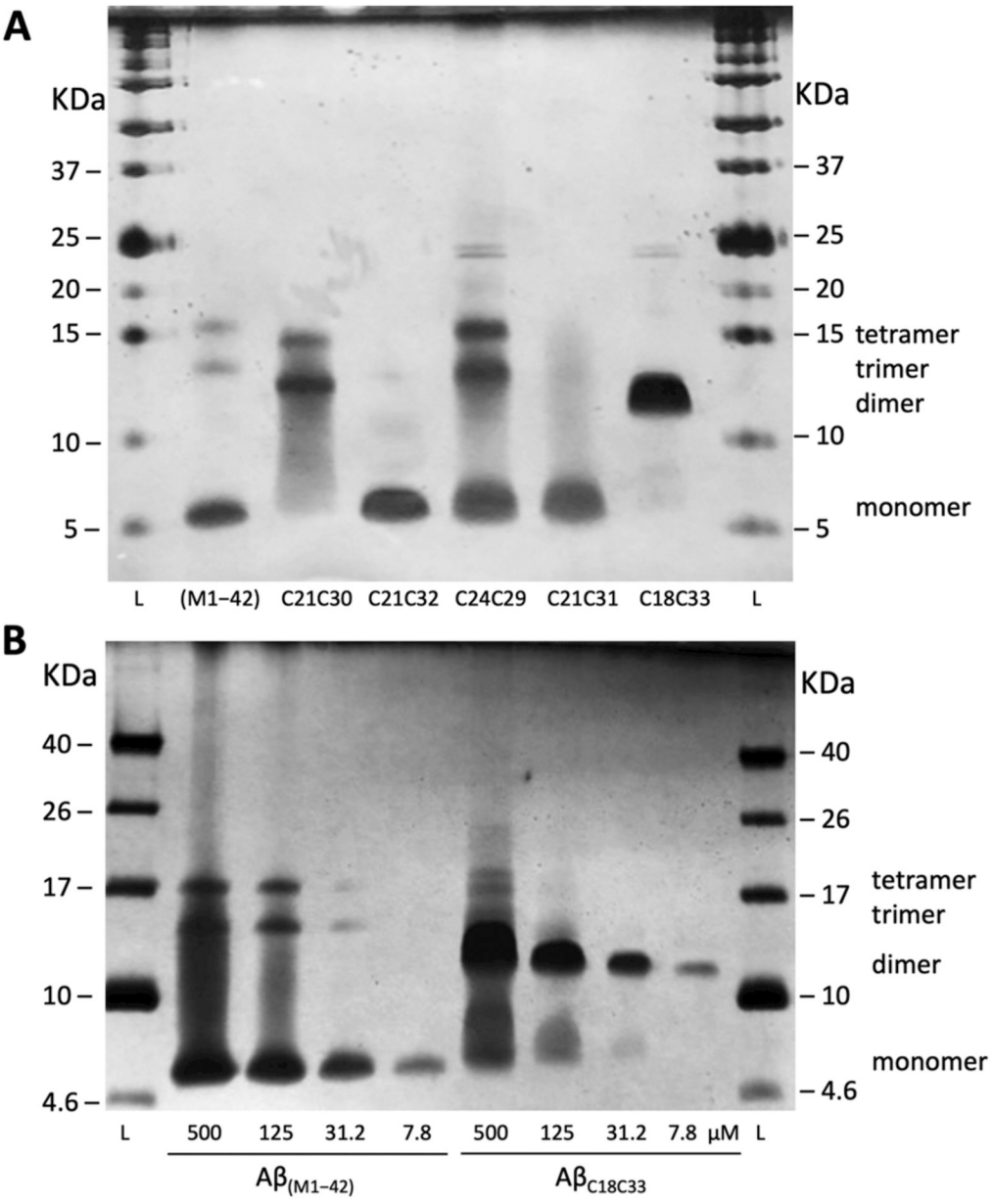

Figure 3.

SDS-PAGE studies of the oligomerization propensities of the disulfide-stabilized Aβ peptides. (A) Oligomerization patterns of disulfide-stabilized Aβ peptides at 80 μM concentration. A 10-μL aliquot of each peptide was run on the gel. (B) Comparison of the oligomerization patterns of $A\beta_{(M1–42)}$ and $A\beta_{C18C33}$ at various concentrations. A 10-μL aliquot of each peptide was run on the gel.

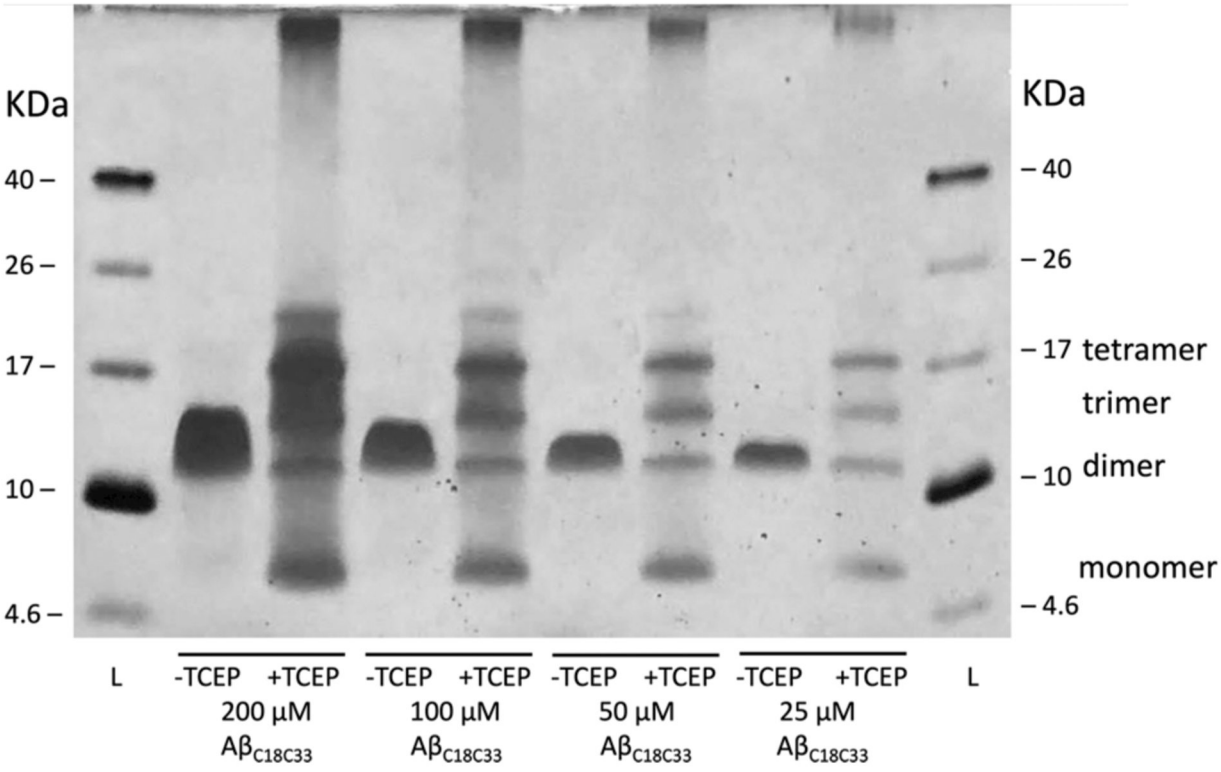

Figure 4.

SDS-PAGE studies of $A\beta_{C18C33}$ before and after TCEP reduction at various concentrations (200, 100, 50, and 25 μM). A 10-μL aliquot of each peptide was run on the gel.

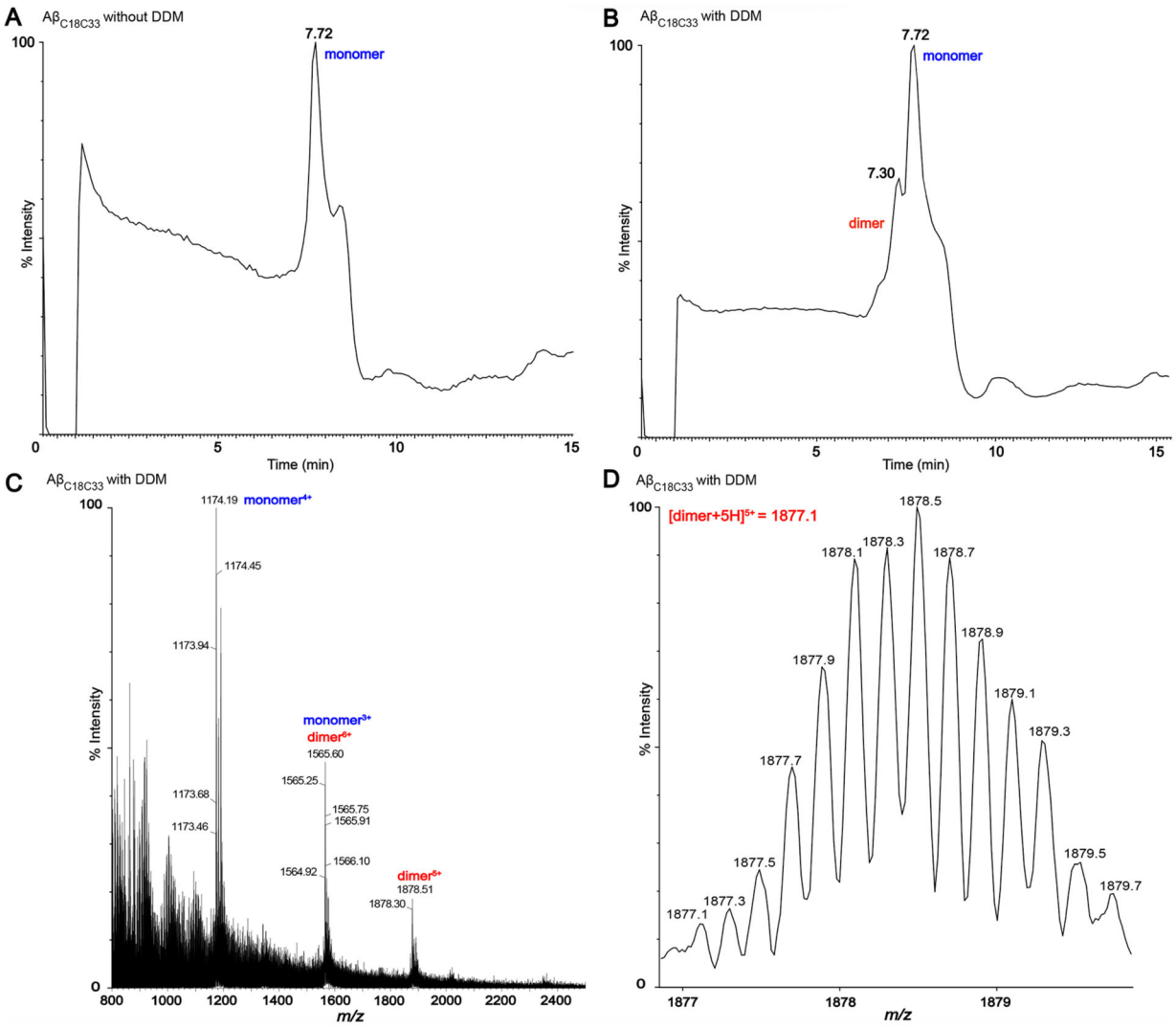

Figure 5.

SEC-MS studies of $A\beta_{C18C33}$. (A) SEC chromatogram showing $A\beta_{C18C33}$ monomers. (B) SEC chromatogram showing the formation of $A\beta_{C18C33}$ dimer after incubation with DDM. (C) Mass spectrum of the SEC peaks corresponding to $A\beta_{C18C33}$ dimer and monomer. (D) Mass peak corresponding to the 5+ ion associated with $A\beta_{C18C33}$ dimer. The Aβ peptide was dissolved in 10 mM ammonium acetate buffer with or without 400 μM DDM (pH 7.3) to a final peptide concentration of 0.25 mg/mL and incubated at 37 °C for 2 hours. SEC-MS was run in 1:1 ammonium formate: acetonitrile running buffer (pH 10.0).

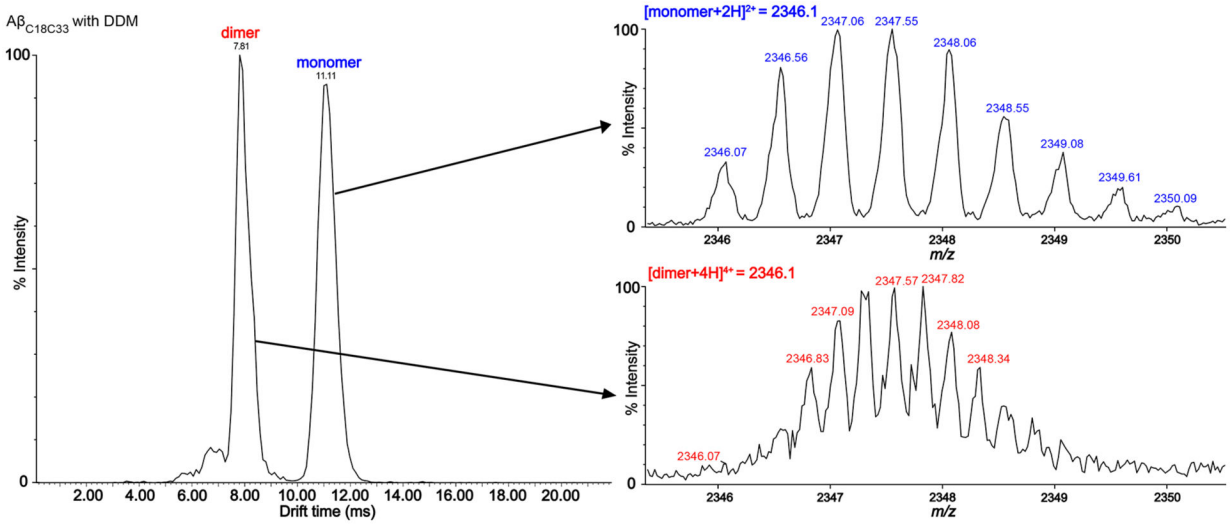

Figure 6.

IM-MS studies of $A\beta_{C18C33}$ in the presence of DDM. The Aβ peptide was dissolved in 200 mM ammonium acetate buffer containing 300 μM DDM (pH 7.4) to a final concentration of 25 μM, then directly injected on the IM-MS system at 100 μL/min.

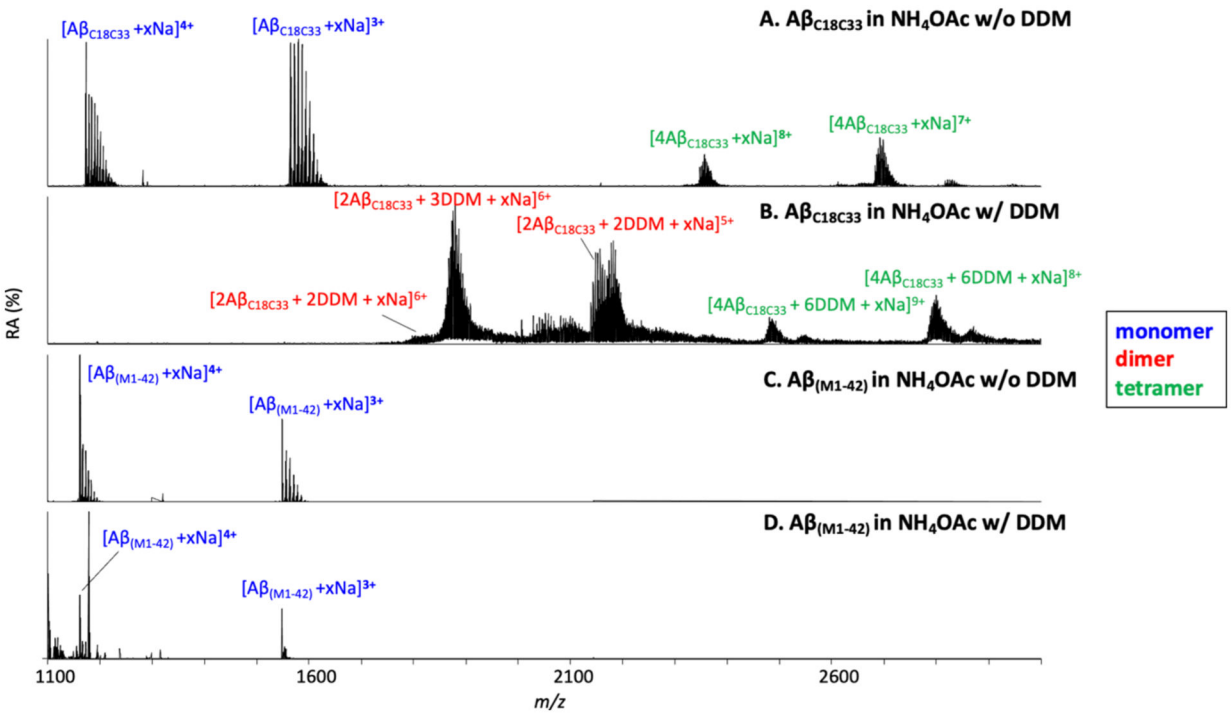

Figure 7.

High-resolution native mass spectrometric analysis of $A\beta_{C18C33}$ and $A\beta_{(M1–42)}$ in the absence or presence of DDM. (A) $A\beta_{C18C33}$ (25 μM) in 200 mM ammonium acetate solution. (B) $A\beta_{C18C33}$ (25 μM) in 200 mM ammonium acetate solution with 300 μM DDM. (C) $A\beta_{(M1–42)}$ (25 μM) in 200 mM ammonium acetate solution. (D) $A\beta_{(M1–42)}$ (25 μM) in 200 mM ammonium acetate solution with 300 μM DDM. Spectra were acquired at a resolution setting of 100,000.

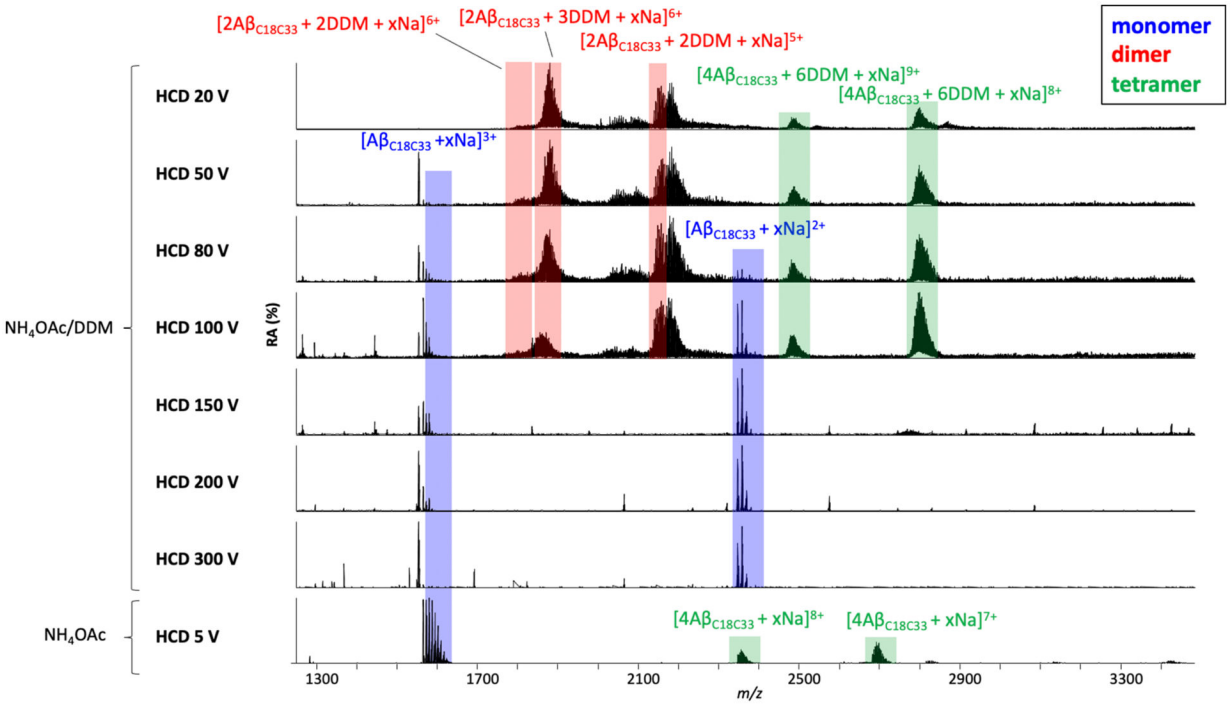

Figure 8.

Native mass spectra of 25 μM Aβ$_{C18C33}$ in 200 mM ammonium acetate with 300 μM DDM as a function of HCD (CID) collision energy and comparison to the native spectrum from ammonium acetate. Spectra were acquired at a resolution setting of 100,000.

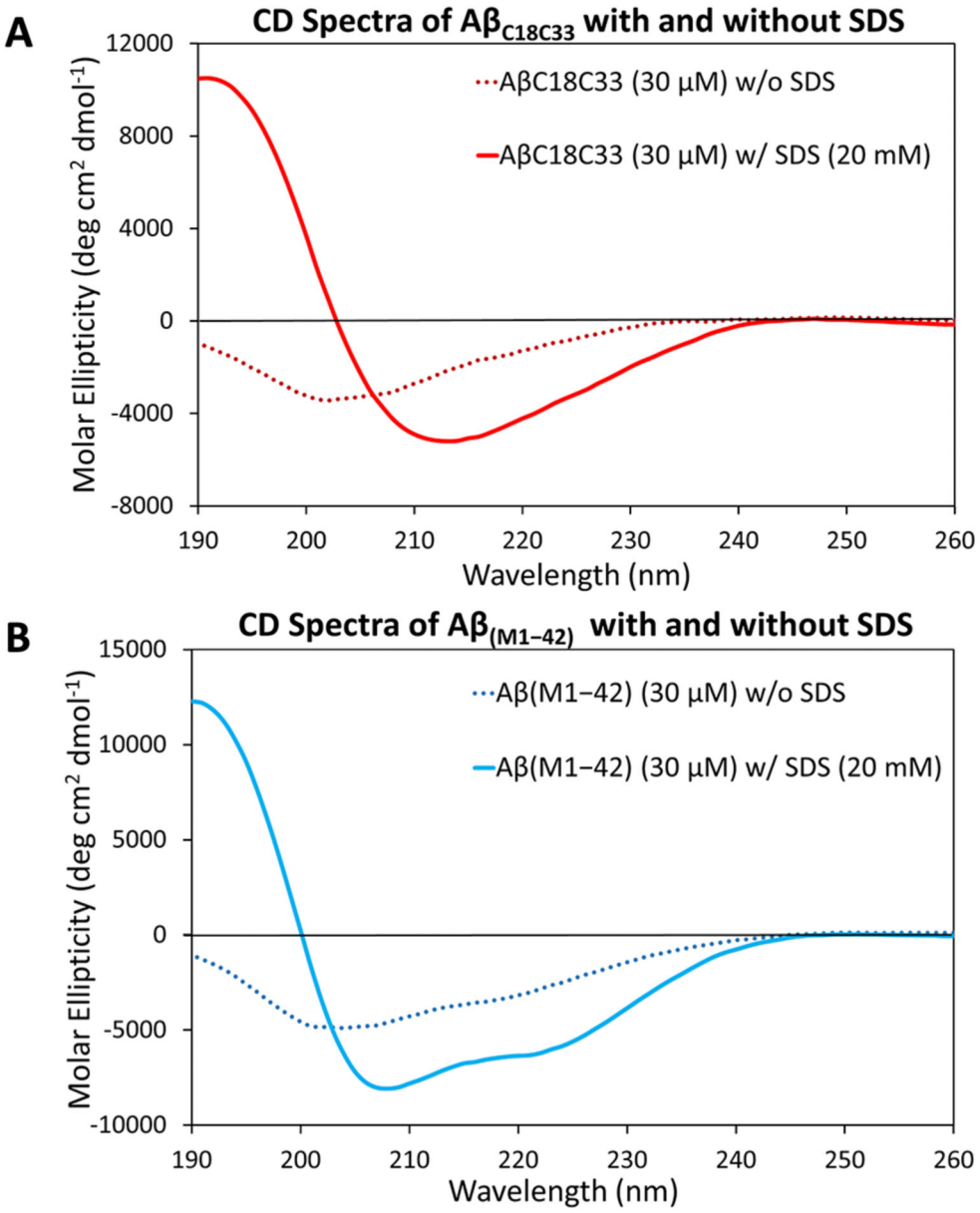

Figure 9.

CD spectra of (A) $A\beta_{C18C33}$ and (B) $A\beta_{(M1–42)}$ in the absence or presence of SDS. CD experiments were performed in 10 mM sodium phosphate buffer at pH 7.4.

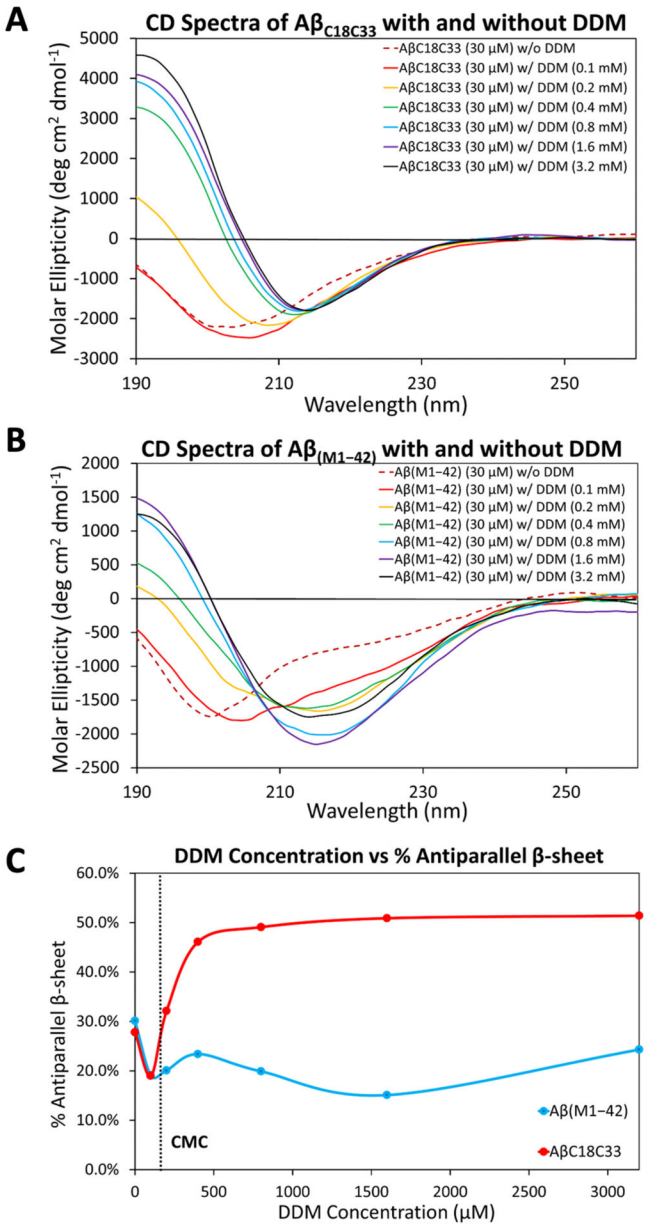

Figure 10.

CD spectra of Aβ$_{C18C33}$ and Aβ$_{(M1–42)}$ with DDM. (A) CD spectra of Aβ$_{C18C33}$ with various concentrations of DDM. (B) CD spectra of Aβ$_{(M1–42)}$ with various concentrations of DDM. CD experiments were performed in 1O mM sodium phosphate buffer at pH 7.4. (C) Percentage of antiparallel β-sheet structure calculated for the Aβ$_{C18C33}$ and Aβ$_{(M1–42)}$ peptides with various concentrations of DDM. The CD spectra were analyzed using the secondary structure analysis server BeStSel.[72,73] The critical micelle concentration (CMC) of DDM (ca. 0.17 mM) is marked with a dashed line.

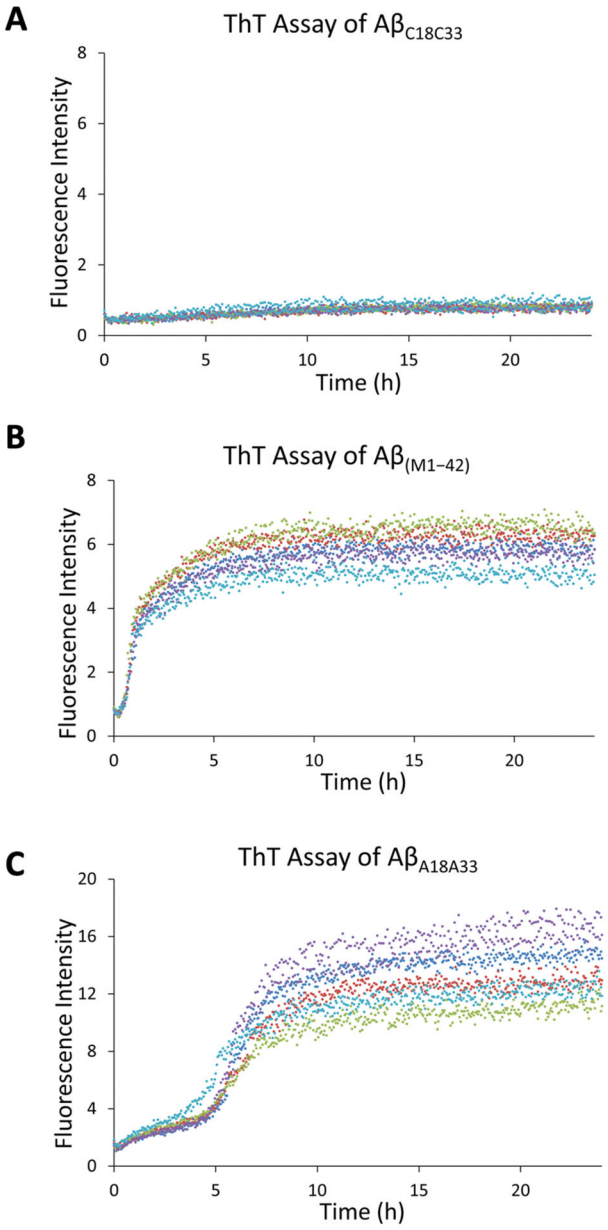

Figure 11.

ThT fluorescence assays of (A) Aβ$_{C18C33}$, (B) Aβ$_{(M1–42)}$, and (C) Aβ$_{A18A33}$. Assays were performed with 40 μM Aβ and 40 μM ThT in pH 7.4 PBS buffer at 37 °C without shaking (quiescent conditions). Fluorescence was monitored with 440 nm excitation and 485 nm emission. The ThT assays were performed in five technical replicates (purple, dark blue, red, light blue, and green).

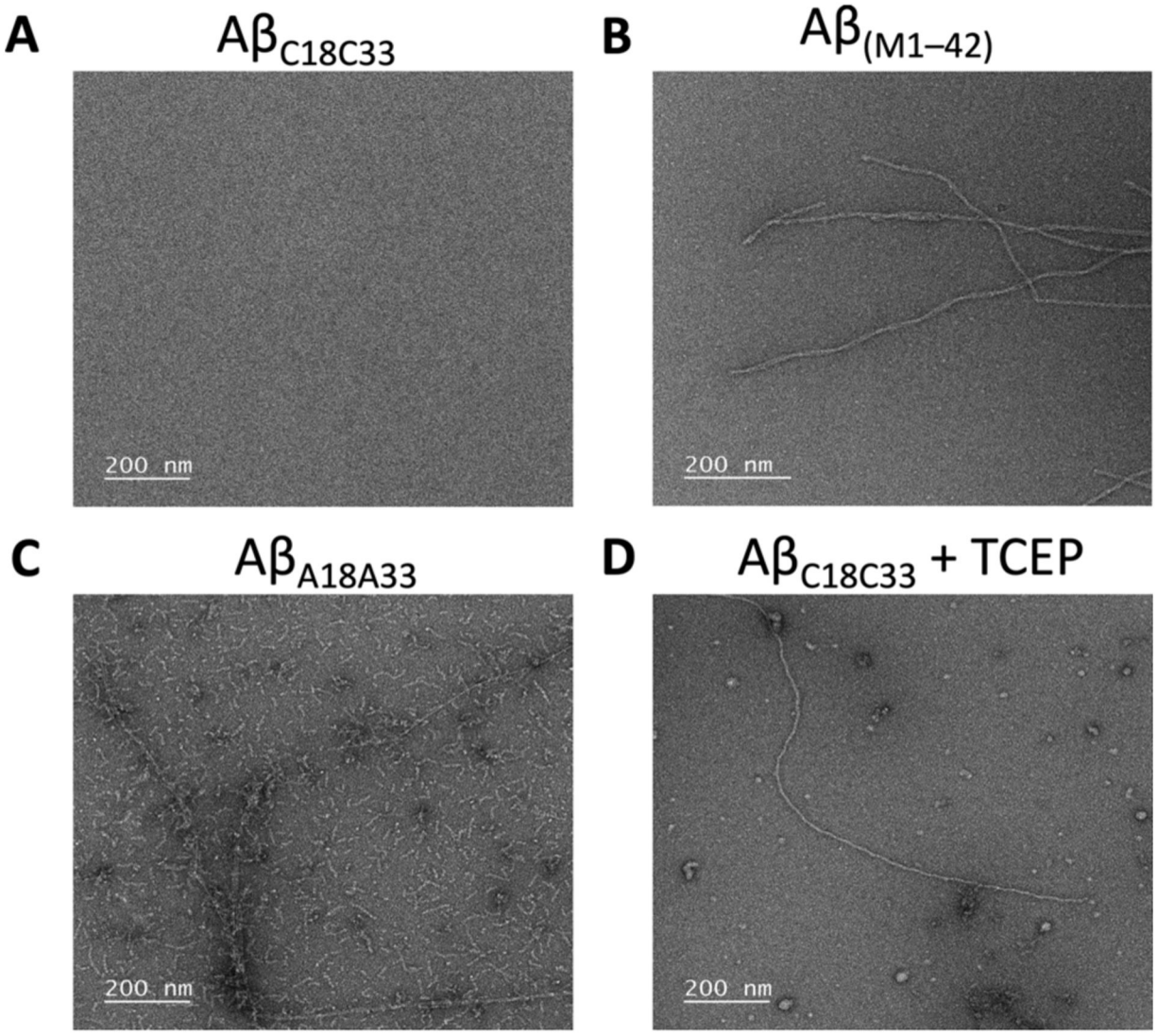

Figure 12.

Transmission electron micrographs of Aβ peptides: (A) $A\beta_{C18C33}$, (B) $A\beta_{(M1-42)}$, (C) $A\beta_{A18A33}$, and (D) $A\beta_{C18C33}$ with TCEP reduction. Solutions of the Aβ peptides were incubated in pH 7.4 PBS buffer for 24 hours at 37 °C and then imaged by TEM with uranyl acetate staining.

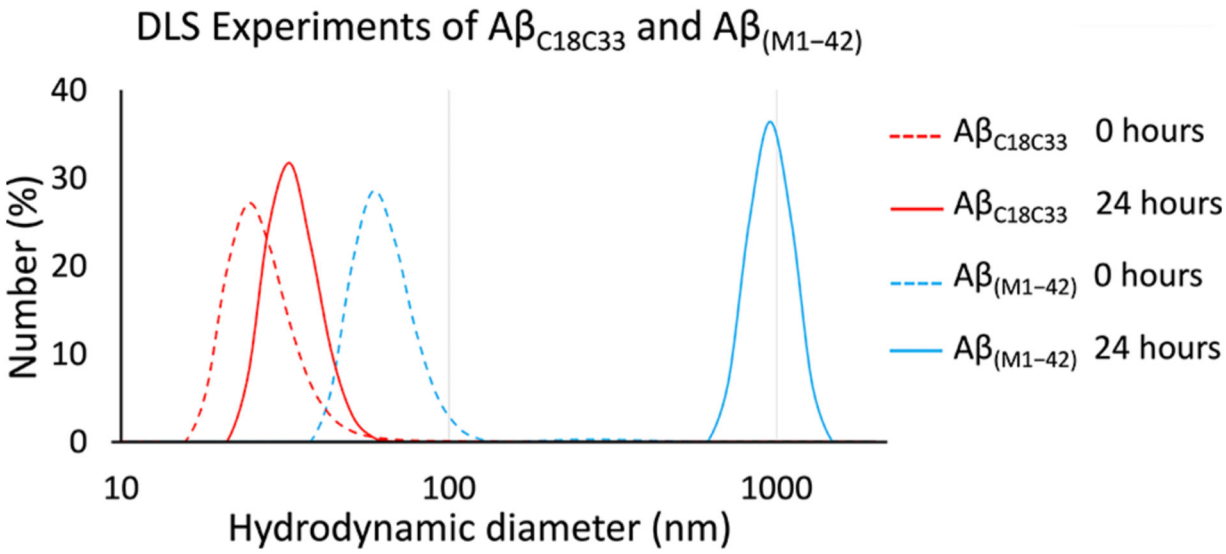

Figure 13.

Dynamic light scattering experiments of $A\beta_{C18C33}$ and $A\beta_{(M1–42)}$. DLS experiments were performed on 30 μM solutions of the Aβ peptides in 10 mM sodium phosphate buffer at pH 7.4. DLS data were recorded for freshly prepared solutions, and then after the solutions were incubated for 24 hours at 37 °C.

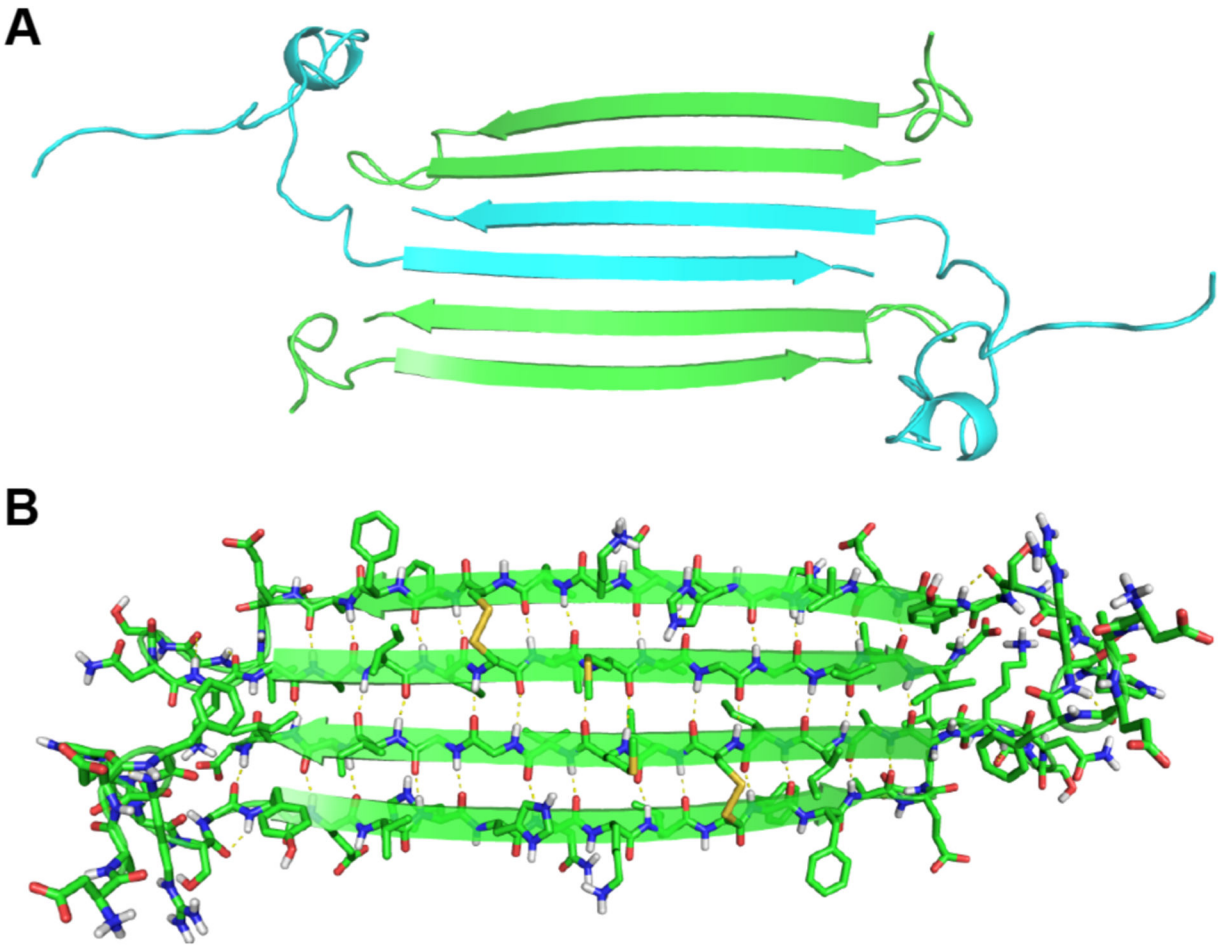

Figure 14.

Structural model of the $A\beta_{C18C33}$ dimer. (A) The recently published NMR structure of an $A\beta_{42}$ tetramer by Carulla and coworkers (PDB 6RHY).[58] (B) Working model for the structure of the $A\beta_{C18C33}$ dimer.